CHAPTER 05

# Compound semiconductor photosensors

# Compound semiconductor photosensors

Compound semiconductor photosensors are opto-semiconductors made of two or more elements mainly from groups II to VI. These photosensors have different spectral response ranges depending on the elements comprising them. This means photosensors can be made that are sensitive to different wavelengths from the ultraviolet to infrared region.

HAMAMATSU provides detectors for many different wavelengths by taking advantage of its expertise in compound semiconductor technology accumulated over many years. We offer an especially wide detector product lineup in the infrared region. Applications for our compound semiconductor photosensors range from academic research to information communication devices and general-purpose electronic equipment.



## Spectral response of compound semiconductor photosensors (typical example)

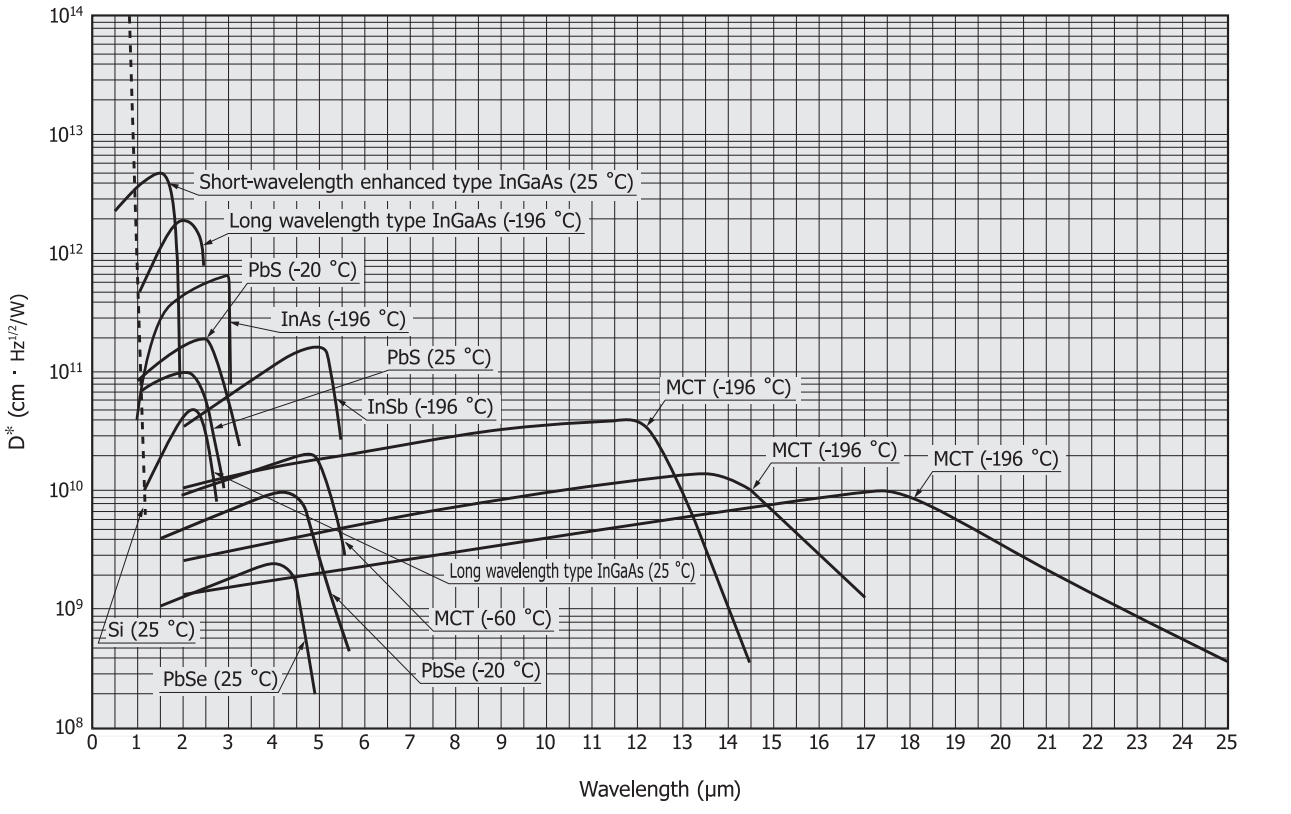


KIRDB0259EF

## ▣ HAMAMATSU compound semiconductor photosensors

| Product name | Spectral response range (μm) | Features |
|---|---|---|
| InGaAs PIN photodiode |   | • Standard type<br>• High-speed response, high sensitivity, low dark current<br>• Various types of active areas, arrays, and packages available |
| |   | • Short-wavelength enhanced type<br>• Can detect light from 0.5 μm |
| |   | • For light measurement around 1.7 μm<br>• TE-cooled type available |
| |   | • For light measurement in water absorption band (1.9 μm)<br>• TE-cooled type available |
| |   | • For NIR spectrometry<br>• TE-cooled type available |
| InGaAs APD |   | • High sensitivity, high-speed response, low dark current<br>• Various sizes of active areas available |
| GaAs PIN photodiode |   | • High-speed response, high sensitivity, low dark current<br>• Arrays and various packages available |

| Product name | | Spectral response range (μm) | Features |
|---|---|---|---|
| PbS photoconductive detector | |   | • Photoconductive detectors whose resistance decreases with input of infrared light<br>• Can be used at room temperatures in a wide range of applications such as radiation thermometers and flame monitors |
| PbSe photoconductive detector | |   | • Detects wavelengths up to 5.2 μm<br>• Offers higher response speed at room temperatures compared to other detectors used in the same wavelength range. Suitable for a wide range of applications such as gas analyzers. |
| InSb photoconductive detector | |   | • Detects wavelengths up to around 6.5 μm, with high sensitivity over long periods of time by thermoelectric cooling |
| InAs photovoltaic detector | |   | • Covers a spectral response range close to PbS but offers higher response speed |
| InSb photovoltaic detector | |   | • High sensitivity in so-called atmospheric window (3 to 5 μm) |
| MCT (HgCdTe) photoconductive detector | |   | • Various types with different spectral response ranges are provided by changing the HgTe and CdTe composition ratio.<br>• Photoconductive detectors whose resistance decreases with input of infrared light<br>• Available with thermoelectric coolers, cryogenic dewars, and stirling coolers |
| MCT (HgCdTe) photovoltaic detector | |   | • High-speed response, low noise |
| Two-color detector | Si + PbS |   | • Wide spectral response range from UV to IR<br>• Incorporates an infrared-transmitting Si photodiode mounted over a PbS detector or PbSe detector or InGaAs PIN photodiode along the same optical axis |
| | Si + PbSe |   | |
| | Si + InGaAs |   | |
| Photon drag detector | |   | • High-speed detector with sensitivity in 10 μm band (for $CO_2$ laser detection)<br>• Room temperature operation with high-speed response |

# 1. InGaAs/GaAs PIN photodiodes

InGaAs PIN photodiodes and GaAs PIN photodiodes are photovoltaic detectors having PN junctions just the same as Si photodiodes.

[Figure 1-1] Spectral response (InGaAs/GaAs PIN photodiodes)

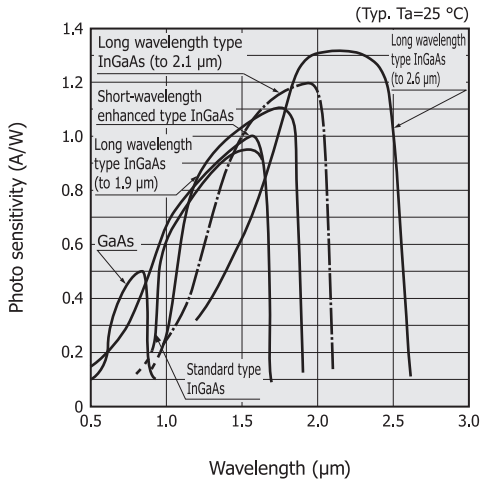


KIRDB0332EC

InGaAs has a smaller band gap energy compared to Si, so it is sensitive to longer wavelengths. Since the InGaAs band gap energy varies depending on the composition ratio of In and Ga [Figure 1-2], infrared detectors with different spectral response ranges can be fabricated by just changing this composition ratio. HAMAMATSU provides standard types having a cut-off wavelength of 1.7 µm, short-wavelength enhanced types, and long wavelength types having a cut-off wavelength extending to 1.9 µm or 2.1 µm or up to 2.6 µm.

[Figure 1-2] $In_{1-x}Ga_xAs$ lattice constant vs. band gap energy

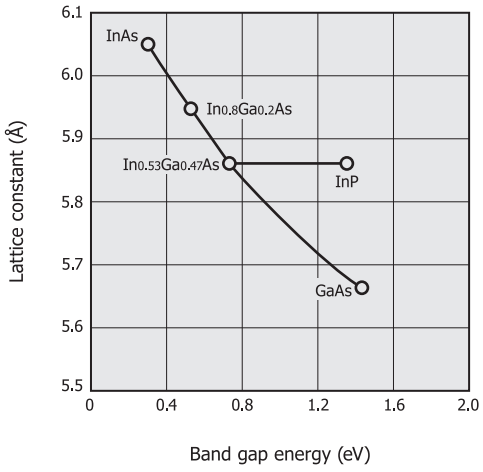


KIRDB0130EA

## 1 - 1 Characteristics

### Current vs. voltage characteristics

When voltage is applied to an InGaAs/GaAs PIN photodiode in a dark state, a current vs. voltage characteristic like that shown in Figure 1-3 (a) is obtained. When light enters the photodiode, this curve shifts as shown at ② in Figure 1-3 (b). As the light level is increased, the curve further shifts as shown at ③ . Here, when both terminals of the photodiode are left open, an open circuit voltage (Vop) appears in the forward direction. When both terminals are shorted, a short circuit current (Isc) flows in the reverse direction.

Figure 1-4 shows methods for measuring the light level by detecting the photocurrent. In Figure 1-4 (a), a load resistor is connected and the voltage Io × RL is amplified by an amplifier having a gain of G. In this circuit, the linearity range is limited [as shown in Figure 1-3 (c)].

Figure 1-4 (b) shows a circuit connected to an op amp. If we set the open-loop gain of the op amp as A, then the equivalent input resistance becomes Rf/A due to negative feedback circuit characteristics. This resistance is several orders of magnitude smaller than the input resistance of the circuit in Figure 1-4 (a), allowing ideal measurement of the short circuit current (Ish). If the short circuit current must be measured over a wide range, then change the Rf as needed.

[Figure 1-3] Current vs. voltage characteristics

(a) In dark state

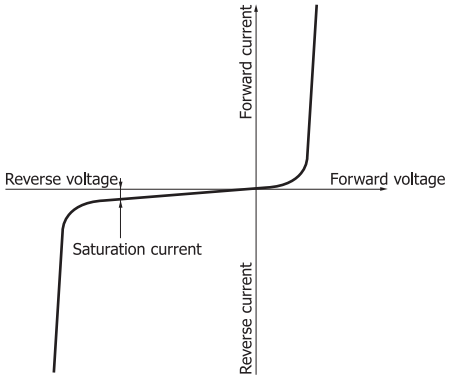


KIRDC0030EA

(b) When light is incident

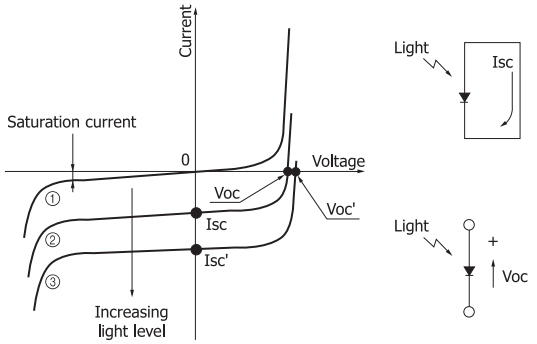


KPDC0005EA

(c) Current vs. voltage characteristics and load line

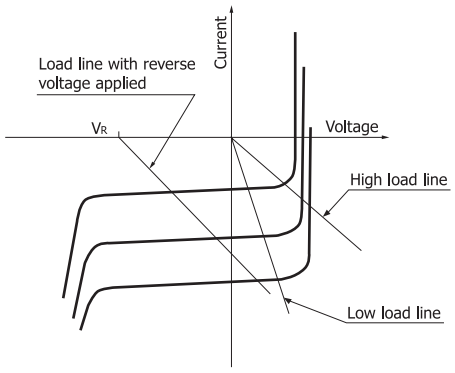


KPDB0003EA

[Figure 1-4] Connection examples

(a) When load resistor is connected

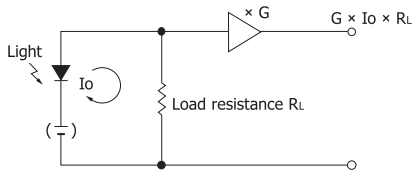


(b) When op amp is connected

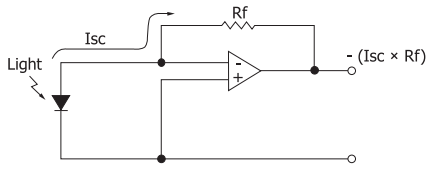


KPDC0006EC

## Equivalent circuit

A circuit equivalent to an InGaAs/GaAs PIN photodiode is shown in Figure 1-5. The short circuit current (Isc) is expressed by equation (1). The linearity limit of the short circuit current is determined by the 2nd and 3rd terms of this equation.

$$Isc = I_L - Is\left[\exp\frac{q\,(Isc \times Rs)}{k\,T} - 1\right] - \frac{Isc \times Rs}{Rsh} \quad \cdots\cdots\cdots (1)$$

$I_L$ : current generated by incident light (proportional to light level)
Is : photodiode reverse saturation current
q : electron charge
Rs : series resistance
k : Boltzmann's constant
T : absolute temperature of photodiode
Rsh: shunt resistance

[Figure 1-5] Equivalent circuit (InGaAs/GaAs PIN photodiode)

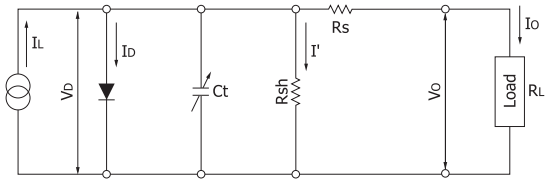


$V_D$: voltage across diode
$I_D$ : diode current
Ct: terminal capacitance
I' : shunt resistance current
Vo: output voltage
Io : output current

KPDC0004EA

## Linearity

The lower limit of InGaAs/GaAs PIN photodiode linearity is determined by noise while the upper limit is determined by the chip structure and composition, active area size, and electrode structure, etc. To expand the upper limit, a reverse voltage is applied in some cases. However, applying 1 V is sufficient if only the linearity needs to be considered. Figure 1-7 shows a connection example for applying a reverse voltage. Although applying a reverse voltage is useful to improve the linearity or response characteristics, it also results in larger dark current and a higher noise level. Excessive reverse voltages might also damage or deteriorate the photodiode, so always use the reverse voltage that is within the absolute maximum rating and set the polarity so that the cathode is at positive potential relative to the anode.

[Figure 1-6] Linearity

(a) InGaAs PIN photodiodes

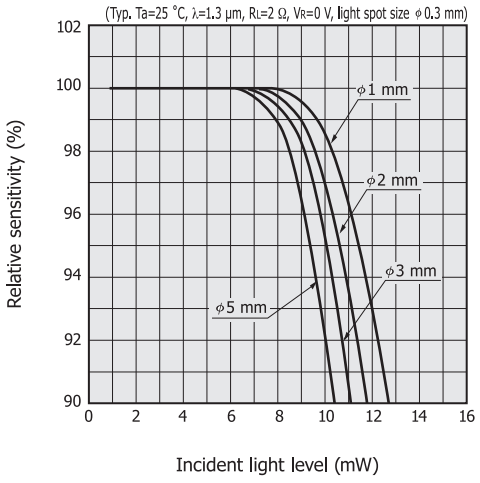


KIRDB0333EB

(b) GaAs PIN photodiode

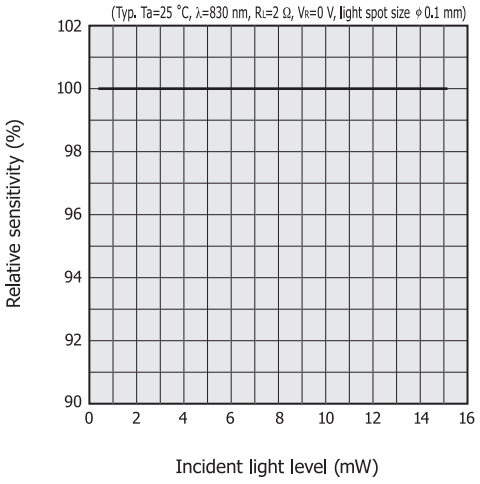


KGPDB0060EA

[Figure 1-7] Connection examples (with reverse voltage applied)

(a) When load resistor is connected

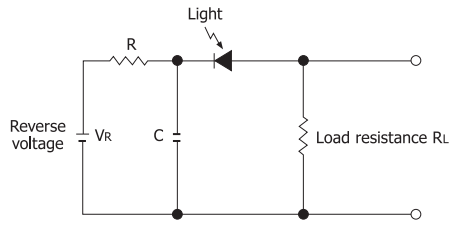


(b) When op amp is connected

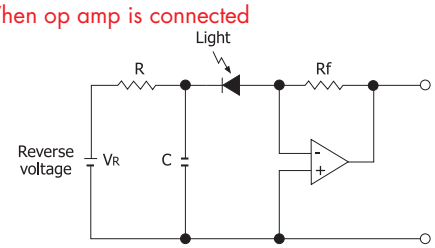


KPDC0008EB

## Noise characteristics

Like other typical photosensors, the lower limits of light detection for InGaAs/GaAs PIN photodiodes are determined by their noise characteristics. Noise current (in) in a photodiode is the sum of the thermal noise current or Johnson noise current (ij) of a resistor, which approximates the shunt resistance Rsh, and the shot noise currents ($i_{SD}$ and $i_{SL}$) resulting from the dark current and the photocurrent, respectively.

$$in = \sqrt{ij^2 + i_{SD}^2 + i_{SL}^2} \ [A] \quad \cdots\cdots\cdots (2)$$

If a reverse voltage is not applied as in Figure 1-4, then ij is given by equation (3).

$$ij = \sqrt{\frac{4k\,T\,B}{Rsh}} \ [A] \quad \cdots\cdots\cdots (3)$$

k : Boltzmann's constant
T: absolute temperature of photodiode
B: noise bandwidth

When a reverse voltage is applied as in Figure 1-7, then there is always a dark current and the $i_{SD}$ is as shown in equation (4).

$$i_{SD} = \sqrt{2q\,I_D\,B} \ [A] \quad \cdots\cdots\cdots (4)$$

q : electron charge
$I_D$: dark current

If photocurrent ($I_L$) is generated by incident light and $I_L >> 0.026/Rsh$ or $I_L >> I_D$, then the shot noise current resulting from the photocurrent is a predominant source of noise current expressed by equation (5).

$$in \simeq i_{SL} = \sqrt{2q\,I_L\,B} \ [A] \quad \cdots\cdots\cdots (5)$$

The amplitude of these noise sources are each proportional to the square root of noise bandwidth (B) and so are expressed in units of $A/Hz^{1/2}$ normalized by B.
The lower limit of light detection for photodiodes is usually expressed as the intensity of incident light required to generate a current equal to the noise current as expressed in equation (3) or (4), which is termed the noise equivalent power (NEP).

$$NEP = \frac{in}{S} \ [W/Hz^{1/2}] \quad \cdots\cdots\cdots (6)$$

in: noise current
S : photo sensitivity

In the circuit shown in Figure 1-7 (b), noise from the op amp and Rf must be taken into account along with the photodiode noise described above. Moreover, in high-frequency regions the transfer function including capacitive components such as photodiode capacitance (Ct) and feedback capacitance (Cf) must also be considered. The lower limit of light detection will be larger than the NEP defined in equation (6) because there are effects from the amplifier's temperature drift and flicker noise in low-frequency regions, gain peaking described later on, and others.
In the case of InGaAs PIN photodiodes, cooled types are often used to improve the lower limit of light detection. Periodically turning the incident light on and off by some means and synchronously detecting only signals of the same frequency are also effective in removing noise from unwanted bands. This allows the detection limit to approach the NEP [Figure 1-8].

[Figure 1-8] Synchronous measurement method

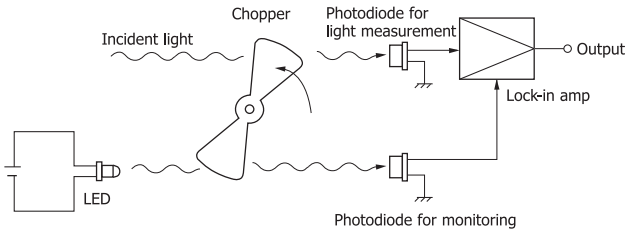


KPDC0007EA

## Spectral response

InGaAs PIN photodiodes are roughly divided into the following three types according to their spectral response ranges.

- Standard type: sensitive in a spectral range from 0.9 to 1.7 µm
- Long wavelength type: sensitive in a spectral range extending to longer wavelengths than standard type
- Short-wavelength enhanced type: variant of the standard type and having extended sensitivity to shorter wavelengths

The cut-off wavelength (λc) on the long wavelength side of photodiodes is expressed by equation (7) using their band gap energy (Eg).

$$\lambda c = \frac{1.24}{Eg} \ [\mu m] \quad \cdots\cdots\cdots (7)$$

Eg: band gap energy [eV]

The InGaAs light absorption layer in the standard type and

short-wavelength enhanced type has a band gap energy of 0.73 eV. In the long wavelength type, this band gap energy is reduced by changing the ratio of elements making up the InGaAs light absorption layer in order to extend the cut-off wavelength to the longer wavelength side.

InGaAs PIN photodiodes require a semiconductor layer called the cap layer which is formed on the InGaAs light absorption layer to suppress the surface leakage current that can cause noise. Light at wavelengths shorter than the cut-off wavelength of the semiconductor comprising the cap layer is almost totally absorbed by the cap layer and so does not reach the light absorption layer, and therefore does not contribute to sensitivity. In the short-wavelength enhanced type, this cap layer is thinned to less than 1/10th the cap layer thickness for the standard type by improving the wafer structure and wafer process. This reduces the amount of light absorbed by the cap layer and so increases the amount of light reaching the light absorption layer, improving the sensitivity at short wavelengths. Because the band gap energy increases as the temperature is lowered, the spectral response range of InGaAs PIN photodiodes shifts to the shorter wavelength side as the photodiode temperature decreases. This also reduces the amount of noise, so D* (detectivity) increases [Figure 1-10].

[Figure 1-9] Spectral response

(a) InGaAs PIN photodiode (standard type)

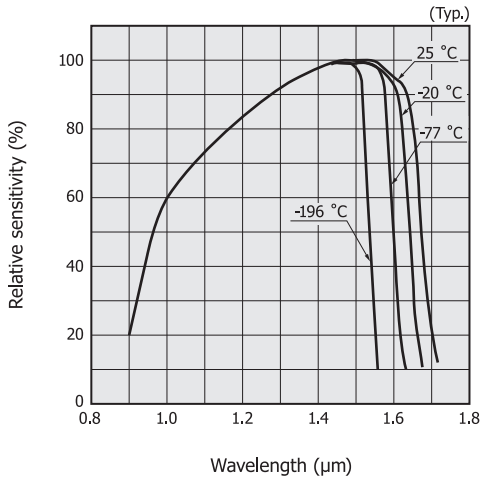


(b) InGaAs PIN photodiode (short-wavelength enhanced type)

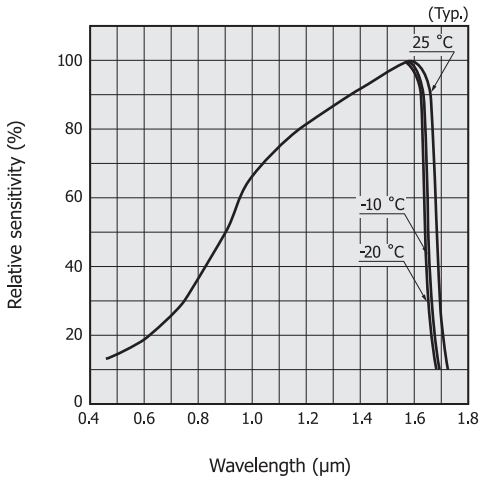


(c) InGaAs PIN photodiode (long wavelength type)

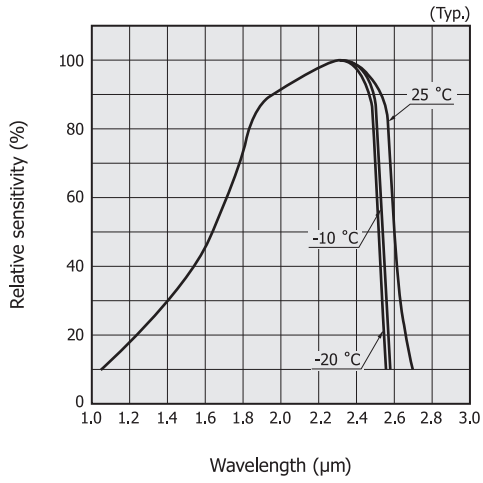


(d) GaAs PIN photodiode

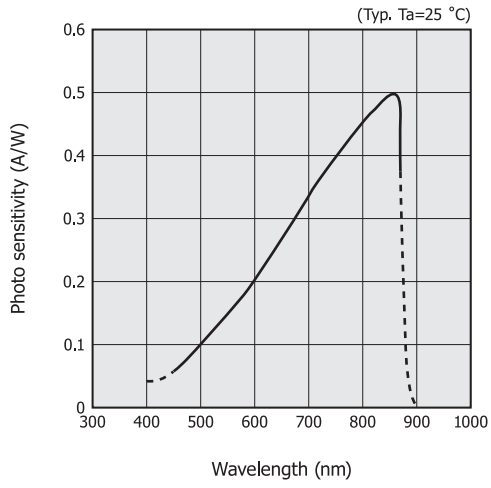

[Figure 1-10] D* vs. wavelength (InGaAs PIN photodiode)
(a) Standard type

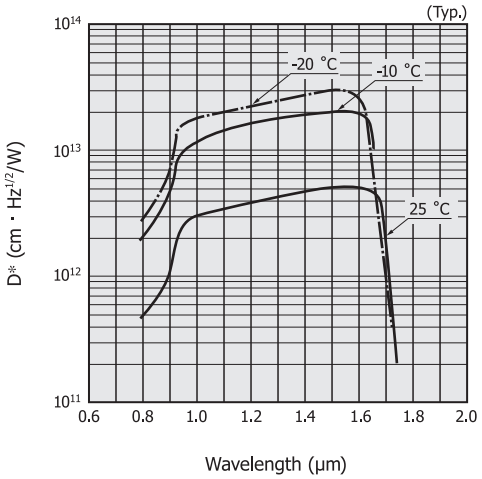


KIRDB0134EA

(b) Long wavelength type (up to 2.6 μm)

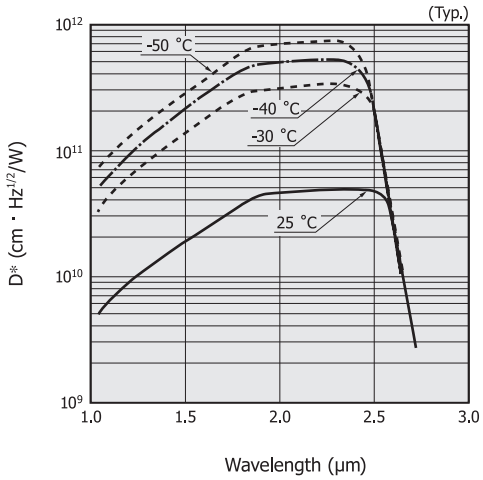


KIRDB0135EA

## Time response characteristics

The time response is a measure of how fast the generated carriers are extracted to an external circuit as output current, and is generally expressed as the rise time or cut-off frequency. The rise time (tr) is the time required for the output signal to rise from 10% to 90% of its peak value and is expressed by equation (8).

$$tr = 2.2Ct\ (R_L + Rs) \quad \cdots\cdots (8)$$

Ct: terminal capacitance
RL: load resistance
Rs: serial resistance

Generally, Rs can be disregarded because RL >> Rs. To make the rise time smaller, the Ct and RL should be lowered, but RL is determined by an external factor and so cannot freely be changed. Ct is proportional to the active area (A) and is inversely proportional to the square root of the reverse voltage (VR).

$$Ct \propto \frac{A}{\sqrt{V_R}} \quad \cdots\cdots (9)$$

Higher response speeds can be obtained by applying a reverse voltage to a photodiode with a small active area.
Charges generated by light absorbed outside the PN junction sometimes takes several microseconds or more to diffuse and reach the electrode. When the time constant of Ct × RL is small, this diffusion time determines response speeds. In applications requiring fast response, be careful not to allow light to strike outside the active area.
The approximate relationship between the rise time tr (unit: s) and cut-off frequency fc (unit: Hz) is expressed by equation (10).

$$tr = \frac{0.35}{fc} \quad \cdots\cdots (10)$$

[Figure 1-11] Terminal capacitance vs. reverse voltage
(a) InGaAs PIN photodiode (standard type)

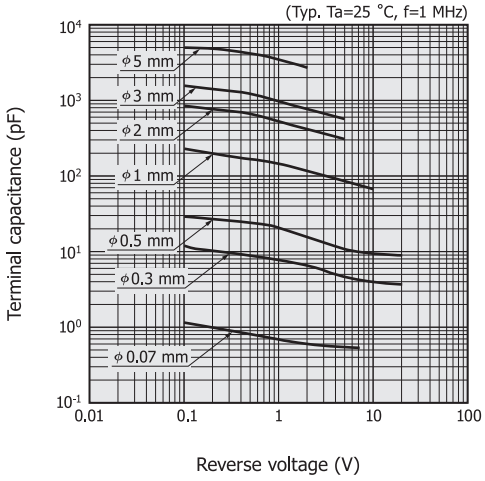


KIRDB0331EC

(b) GaAs PIN photodiode

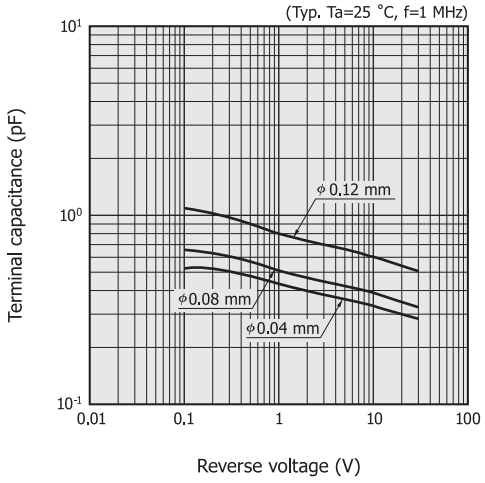


KGPDB0059EA

Figure 1-12 shows a high-speed light detection circuit using an InGaAs PIN photodiode. This is a specific example of a connection based on the circuit shown in Figure 1-7 (a) and uses a 50 Ω load resistance. The ceramic capacitor C is for

reducing the internal resistance of the reverse voltage power supply. The resistor R is for protecting the photodiode, and its value should be selected so that the voltage drop caused by the maximum photocurrent will be sufficiently smaller than the reverse voltage. The photodiode leads, capacitor leads, and coaxial cable wires, etc. carrying high-speed pulses should be kept as short as possible.

[Figure 1-12] High-speed light detection circuit (InGaAs PIN photodiode)

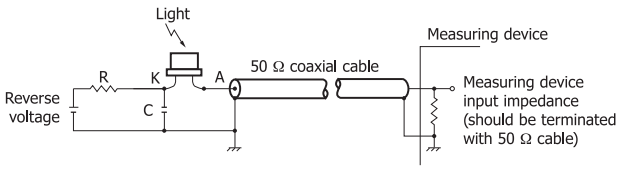


KPDC0009EA

## Temperature characteristics

As described in "Spectral response" in section 1-1, "Characteristics," the spectral response changes with the photodiode temperature. Figure 1-13 shows temperature characteristics of shunt resistance of InGaAs PIN photodiodes. Here, the S/N is improved because the shunt resistance becomes larger as the photodiode temperature decreases. HAMAMATSU provides one-stage and two-stage TE-cooled InGaAs PIN photodiodes that can be used at a constant operating temperature (or by cooling).

[Figure 1-13] Shunt resistance vs. element temperature [InGaAs PIN photodiode (standard type)]

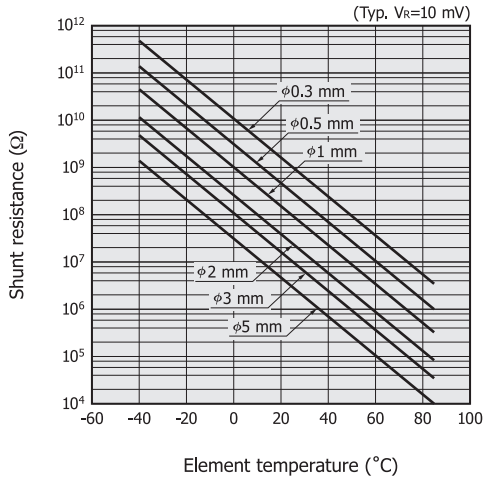


KIRDB0330EA

# 1-2 How to use

## Connection to an op amp

A connection example is shown in Figure 1-14. The input impedance of the op amp circuit in Figure 1-14 is the value of the feedback resistance Rf divided by the open loop gain and so is very small. This yields excellent linearity.

[Figure 1-14] Connection example

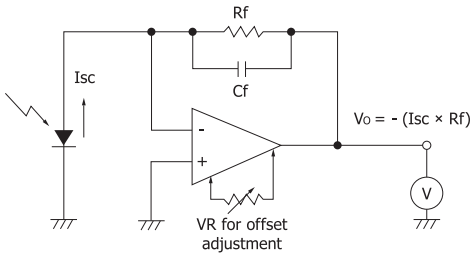


KIRDC0040EB

Precautions when using an op amp are described below.

### (1) Selecting feedback resistance

In Figure 1-14, the short circuit current Isc is converted to the output voltage Vo of "Isc × Rf," so the feedback resistance Rf is determined by Isc and Vo. If Rf is larger than the photodiode shunt resistance Rsh, then the op amp's input noise voltage and input offset voltage are multiplied by (1 + Rf/Rsh) and superimposed on the output voltage. The op amp bias current error also increases, so there is a limit to the Rf increase.

The feedback capacitance Cf is also called the dumping capacitance and is mainly used to prevent oscillation. A capacitance of several picofarads is sufficient for this purpose.

This feedback circuit has a time constant of Cf × Rf and serves as a noise filter. It also limits the response speed at the same time, so the feedback resistance value must be carefully selected to match the application. Error due to an offset voltage can usually be reduced to less than 1 mV by connecting a variable resistor to the offset adjustment terminals on the op amp.

### (2) Selecting an op amp

The actual input resistance of op amps is limited, so a certain amount of bias current flows in or out through the input terminal. This might cause an error depending on the amplitude of the detected current.

The bias current ranges from several hundred picoamperes to several hundred nanoamperes for bipolar type op amps, although some FET input type op amps exhibit a low bias current of 0.1 picoamperes or less.

In general, the bias current of FET input type op amps doubles for every 10 °C increase in temperature, while the bias current of bipolar type op amps decreases. Because of this, it is also necessary to consider selecting a bipolar type op amp when designing circuits for high temperature applications. Just as with offset voltages, the error voltage due to a bias current can be reduced by connecting a variable resistor to the offset adjustment terminals of the op amp.

# 2. InGaAs APD

InGaAs APDs (avalanche photodiodes) are infrared detectors having an internal multiplication function. When a reverse voltage is applied, they multiply photocurrent to achieve high sensitivity and high-speed response.
InGaAs APDs are sensitive to light in the 1 µm band where optical fibers exhibit low loss, and so are widely used for optical fiber communications. Light in the 1 µm band is highly safe for human eyes (eye safe) and is also utilized for FSO (free space optics) and optical distance measurement.

## 2 - 1 Operating principle

When electron-hole pairs are generated in the depletion layer of an APD with a reverse voltage applied to the PN junction, the electric field created across the PN junction causes the electrons to drift toward the $N^+$ side and the holes to drift toward the $P^+$ side. The drift speed of these carriers depends on the electric field strength. However, when the electric field is increased, the carriers are more likely to collide with the crystal lattice so that the drift speed of each carrier becomes saturated at a certain speed. If the reverse voltage is increased even further, some carriers that escaped collision with the crystal lattice will have a great deal of energy. When these carriers collide with the crystal lattice, ionization takes place in which electron-hole pairs are newly generated. These electron-hole pairs then create additional electron-hole pairs in a process just like a chain reaction. This is a phenomenon known as avalanche multiplication. APDs are photodiodes having an internal multiplication function that utilizes this avalanche multiplication.

[Figure 2-1] Structure and electric field profile (InGaAs APD)

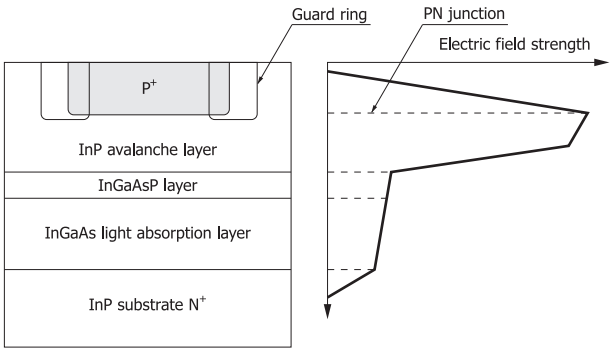


KIRDC0077EA

Because the band gap energy of InGaAs is small, applying a high reverse voltage increases the dark current. To cope with this, InGaAs APDs employ a structure in which the InGaAs light absorption layer that generates electron-hole pairs by absorbing light is isolated from the InP avalanche layer that multiplies carriers generated by light utilizing avalanche multiplication. APDs with this structure for separating the light absorption layer from the avalanche layer are called the SAM (separated absorption and multiplication) type. HAMAMATSU InGaAs APDs employ this SAM type.

## 2 - 2 Characteristics

### Dark current vs. reverse voltage characteristics

APD dark current $I_D$ consists of two dark current components: $I_{DS}$ (surface leakage current, etc. flowing at the interface between the PN junction and the surface passivation film) which is not multiplied, and $I_{DG}$ (recombination current, tunnel current, and diffusion current generated inside the semiconductor, specified at M=1) which is multiplied.

$$I_D = I_{DS} + M \cdot I_{DG} \cdots\cdots (11)$$

Figure 2-2 shows an example of current vs. reverse voltage characteristics for an InGaAs APD. Since the InGaAs APD has the structure shown in Figure 2-1, there is no sensitivity unless the depletion layer extends to the InGaAs light absorption layer at a low reverse voltage.

[Figure 2-2] Dark current and photocurrent vs. reverse voltage (G8931-04)

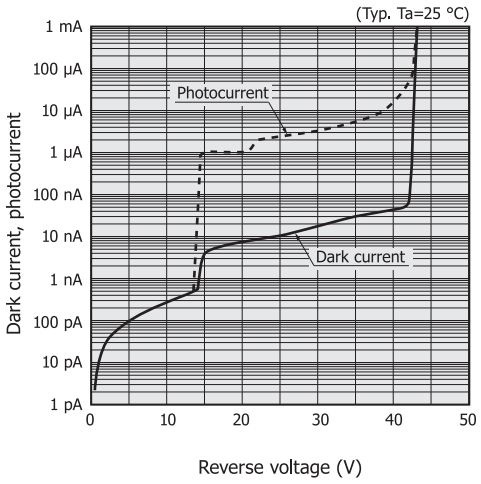


KAPDB0123EA

In our InGaAs APDs, under the condition that they are not irradiated with light, the reverse voltage that causes a reverse current of 100 µA to flow is defined as the breakdown voltage ($V_{BR}$), and the reverse current at a reverse voltage $V_R = 0.9 \times V_{BR}$ is defined as the dark current.

### Gain vs. reverse voltage characteristics

InGaAs APD gain characteristic depends on the electric field strength applied to the InP avalanche layer, so the gain usually increases as the reverse voltage is increased. But increasing the reverse voltage also increases the dark current, and the electric field applied to the InP avalanche layer decreases due

to a voltage drop in the serial resistance component of the photodiode. This means that the gain will not increase even if the reverse voltage is increased higher than that level. If the APD is operated at or near the maximum gain, the voltage drop in the serial resistance component will become large, causing a phenomenon in which photocurrent is not proportional to the incident light level.

[Figure 2-3] Temperature characteristics of gain (G8931-04)

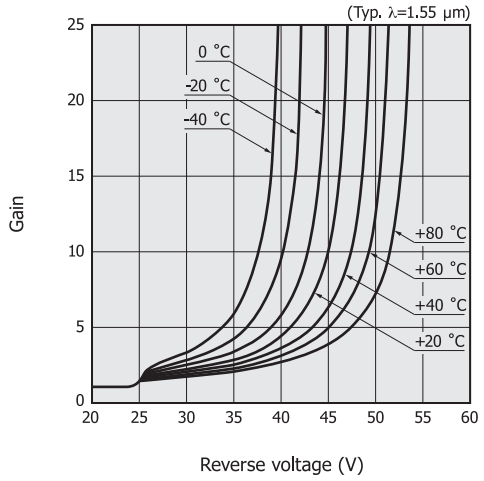


KIRDB0396EA

InGaAs APD gain varies with temperature as shown in Figure 2-3. The gain at a certain reverse voltage becomes smaller as the temperature rises. This phenomenon occurs because the crystal lattice vibrates more heavily as the temperature rises, increasing the possibility that the carriers accelerated by the electric field may collide with the lattice before reaching an energy level sufficient to cause ionization. To obtain a constant output, the reverse voltage must be adjusted to match changes in temperature or to keep the photodiode temperature constant. Figure 2-4 is a graph showing the temperature dependence of dark current vs. reverse voltage characteristics in a range from -40 to +80 °C.

[Figure 2-4] Temperature characteristics of dark current (G8931-04)

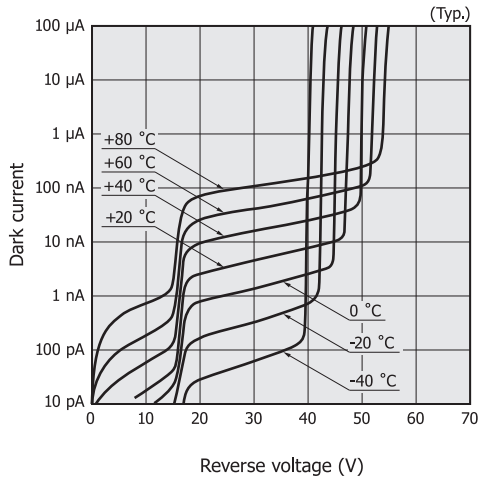


KIRDB0397EA

Temperature characteristic of breakdown voltage is shown in Figure 2-5.

[Figure 2-5] Breakdown voltage vs. temperature (G8931-04)

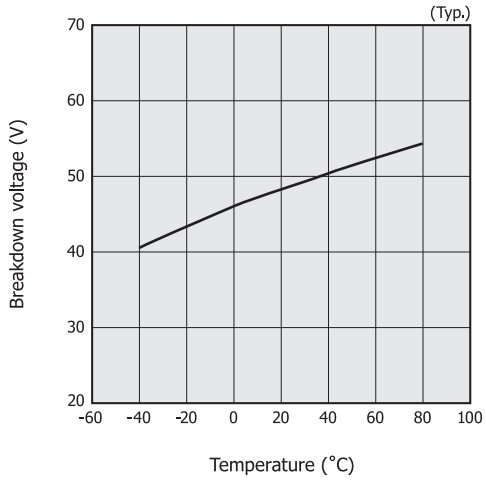


KIRDB0398EA

## Spectral response

When light with energy higher than the band gap energy of the semiconductor is absorbed by the photodiode, electron-hole pairs are generated and detected as signals. The following relationship exists between the band gap energy Eg (unit: eV) and the cut-off wavelength λc (unit: µm), as shown in equation (12).

$$\lambda c = \frac{1.24}{Eg} \text{ [µm]} \quad \cdots\cdots (12)$$

As light absorption material, InGaAs APDs utilize InGaAs whose composition is lattice-matched to InP. The band gap energy of that material is 0.73 eV at room temperature. The InGaAs APD cut-off wavelength is therefore approx. 1.7 µm.
The InGaAs APD spectral response differs depending on the gain [Figure 2-6]. Sensitivity on the shorter wavelength side decreases because short-wavelength light is absorbed by the InP avalanche layer.

[Figure 2-6] Spectral response (G8931-20)

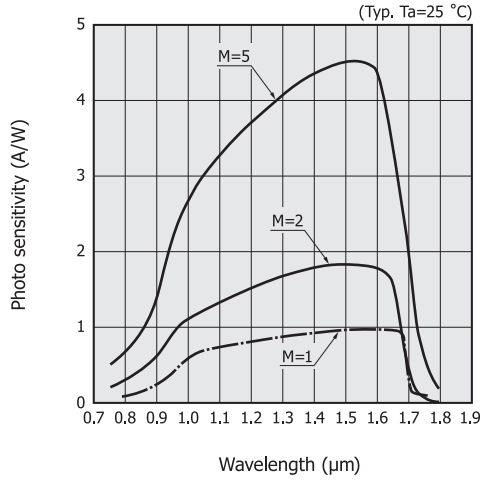


KIRDB0120EB

Temperature characteristics of the InGaAs band gap energy affect temperature characteristics of InGaAs APD spectral response. As the temperature rises, the InGaAs band gap energy becomes smaller, making the cut-off wavelength longer.
InGaAs APDs have an anti-reflection film formed on the light incident surface in order to prevent the quantum efficiency from dropping by reflection on the APD active area surface.

## Terminal capacitance vs. reverse voltage characteristics

The graph curve of terminal capacitance vs. reverse voltage characteristics for InGaAs APDs differs from that of InGaAs PIN photodiodes [Figure 2-7]. This is because their PN junction positions are different.

[Figure 2-7] Terminal capacitance vs. reverse voltage (G8931-04)

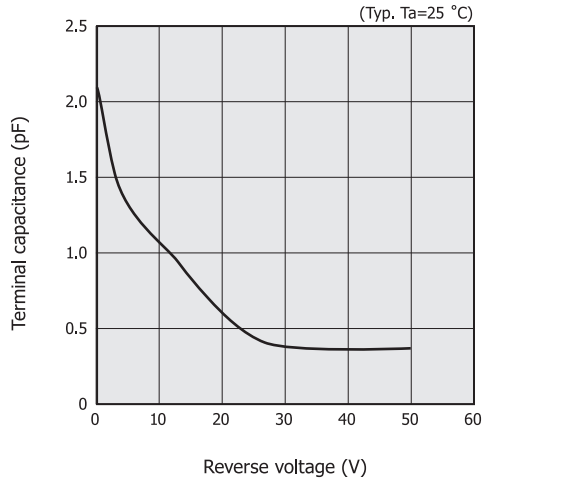


## Noise characteristics

In InGaAs APDs, the gain for each carrier has statistical fluctuations. Multiplication noise known as excess noise is therefore added during the multiplication process. The InGaAs APD shot noise (In) becomes larger than the InGaAs PIN photodiode shot noise, and is expressed by equation (13).

$$In^2 = 2q\,(I_L + I_{DG})\,B\,M^2\,F + 2q\,I_{DS}\,B \quad \cdots\cdots\cdots (13)$$

q : electron charge
$I_L$ : photocurrent at M=1
$I_{DG}$ : dark current component multiplied
$I_{DS}$ : dark current component not multiplied
B : bandwidth
M : gain (multiplication ratio)
F : excess noise factor

The ionization rate is the number of electron-hole pairs generated by a carrier (electron or hole) when it traverses a unit distance in the semiconductor, and is defined as the electron ionization rate α [$cm^{-1}$] and the hole ionization rate β [$cm^{-1}$]. These ionization rates are important parameters that determine the multiplication mechanism. The ratio of β to α is called the ionization rate ratio (k), which is a parameter that indicates the InGaAs APD noise.

$$k = \frac{\beta}{\alpha} \quad \cdots\cdots\cdots (14)$$

The ionization rate ratio is a physical constant inherent to individual semiconductor materials. The ionization rate ratio for InP is k>1 since the hole ionization rate is larger than the electron ionization rate. Therefore, in InGaAs APDs, the holes of the electron-hole pairs generated by light absorption in the InGaAs layer will drift toward the InP avalanche layer due to the reverse voltage.
The excess noise factor (F) is expressed using the ionization rate ratio (k) as in equation (15).

$$F = M\,k + \left(2 - \frac{1}{M}\right)(1 - k) \quad \cdots\cdots\cdots (15)$$

The excess noise factor (F) can also be approximated as $F=M^x$ (x: excess noise index). Figure 2-8 shows an example of the relationship between the InGaAs APD excess noise factor and the gain. In this figure, the excess noise index is approx. 0.7.

[Figure 2-8] Excess noise factor vs. gain (G8931-04, typical example)

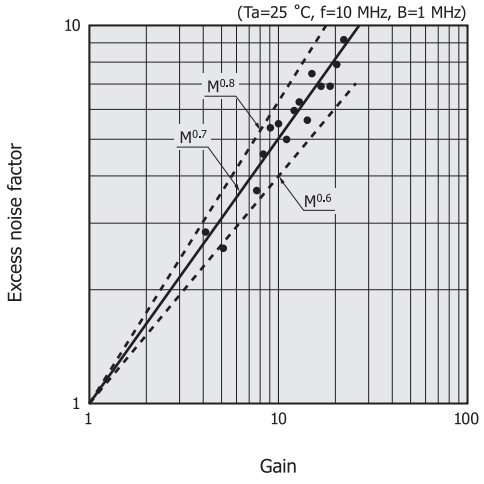


As already explained, InGaAs APDs generate noise accompanying the multiplication process, so excess noise increases as the gain becomes higher. The output signal also increases as the gain becomes higher, so the S/N is maximized at a certain gain. The S/N for an InGaAs APD can be expressed by equation (16).

$$S/N = \frac{I_L^2\,M^2}{2q\,(I_L + I_{DG})\,B\,M^2\,F + 2q\,I_{DS}\,B + \dfrac{4\,k\,T\,B}{R_L}} \quad \cdots\cdots\cdots (16)$$

$2q\,(I_L + I_{DG})\,B\,M^2\,F$: excess noise
$2q\,I_{DS}\,B$: shot noise
k : Boltzmann's constant
T : absolute temperature
$R_L$: load resistance

The optimal gain (Mopt) can be found from conditions that maximize the value of equation (16), and given by equation (17) if $I_{DS}$ is ignored.

$$Mopt = \left[ \frac{4k\,T}{q\,(I_L + I_{DG}) \cdot x \cdot R_L} \right]^{\frac{1}{2+x}} \cdots\cdots\cdots (17)$$

[Figure 2-9] Signal power and noise power vs. gain

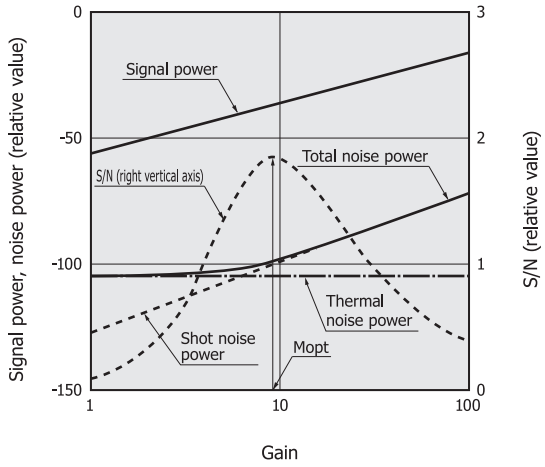


KIRDB0400EA

## Time response characteristics

Major factors that determine the response speed of an APD are the CR time constant, drift time (time required for the carrier to traverse the depletion layer), and the multiplication time. The cut-off frequency determined by the CR time constant is given by equation (18).

$$fc(CR) = \frac{1}{2\pi\, Ct\, R_L} \cdots\cdots\cdots (18)$$

Ct: terminal capacitance
RL: load resistance

To increase the cut-off frequency determined by the CR time constant, the terminal capacitance should be reduced. This means that a smaller active area with a thicker depletion layer is advantageous for raising the cut-off frequency. The relationship between cut-off frequency (fc) and the rise time (tr) is expressed by equation (19).

$$tr = \frac{0.35}{fc(CR)} \cdots\cdots\cdots (19)$$

The drift time cannot be ignored if the depletion layer is made thick. The drift time trd and cut-off frequency fc(trd) determined by the drift time trd are expressed by equations (20) and (21), respectively.

$$trd = \frac{W}{vds} \cdots\cdots\cdots\cdots (20)$$

$$fc(trd) = \frac{0.44}{trd} \cdots\cdots\cdots (21)$$

W : depletion layer thickness
vds: drift speed

The hole drift speed in InGaAs becomes saturated at an electric field strength of approx. $10^4$ V/cm, and the drift speed at that point is approx. $5 \times 10^6$ cm/s. A thinner depletion layer is advantageous in improving the cut-off frequency fc(trd) determined by the drift time, so the cut-off frequency fc(trd) determined by the drift time has a trade-off relation with the cut-off frequency fc(CR) determined by the CR time constant.

The carriers passing through the avalanche layer repeatedly collide with the crystal lattice, so a longer time is required to move a unit distance than the time required to move in areas outside the avalanche layer. The time (multiplication time) required for the carriers to pass through the avalanche layer becomes longer as the gain increases.

In general, at a gain of 5 to 10, the CR time constant and drift time are the predominant factors in determining the response speed, and at a gain higher than 10, the multiplication time will be the predominant factor.

One cause that degrades the response speed in a low gain region is a time delay due to the diffusion current of carriers from outside the depletion layer. This time delay is sometimes as large as a few microseconds and appears more prominently in cases where the depletion layer has not extended enough versus the penetration depth of incident light into the InGaAs.

To achieve high-speed response, it is necessary to apply a reverse voltage higher than a certain level, so that the InGaAs light absorption layer becomes fully depleted. If the InGaAs light absorption layer is not fully depleted, the carriers generated by light absorbed outside the depletion layer might cause “trailing” that degrades the response characteristics.

When the incident light level is high and the resulting photocurrent is large, the attraction force of electrons and holes in the depletion layer serves to cancel out the electric field, so the carrier drift speed in the InGaAs light absorption layer becomes slower and time response is impaired. This phenomenon is called the space charge effect and tends to occur especially when the optical signal is interrupted.

The relationship between the InGaAs APD cut-off frequency and gain is shown in Figure 2-10.

[Figure 2-10] Cut-off frequency vs. gain (G8931-04)

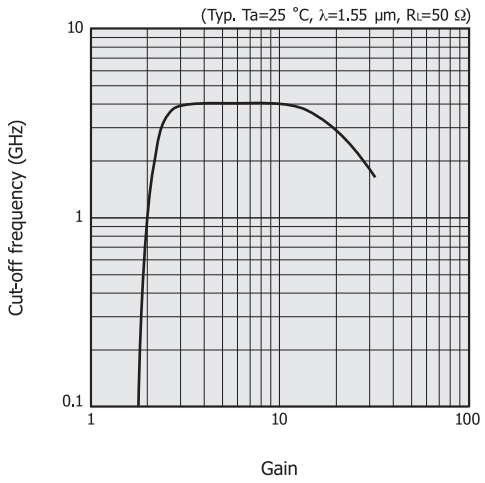


KIRDB0401EA

### Sensitivity uniformity of active area

Since a large reverse voltage is applied to InGaAs APDs to apply a high electric field across the depletion layer, this electric field might concentrate locally especially at or near the junction and tend to cause breakdowns. To prevent this, HAMAMATSU InGaAs APDs use a structure having a guard ring formed around the PN junction. This ensures uniform sensitivity in the active area since the electric field is applied uniformly over the entire active area.

[Figure 2-11] Sensitivity distribution in active area (G8931-20)

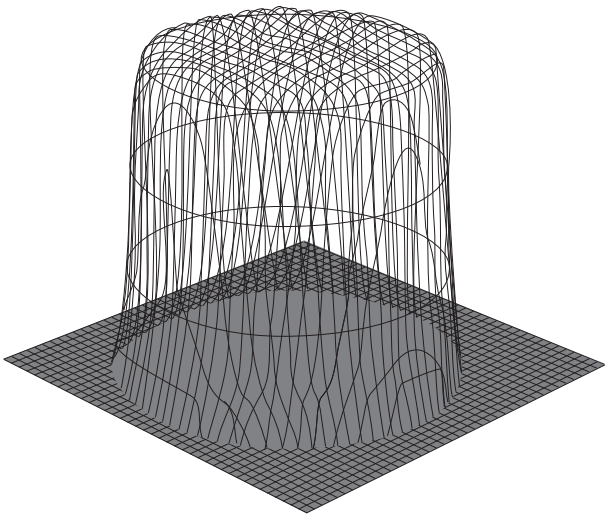

KIRDC0078EA

## 2 - 3 How to use

InGaAs APDs can be handled nearly the same as InGaAs PIN photodiodes and Si APDs. However, the following precautions should be taken.

① The maximum reverse current for InGaAs APDs is 2 mA. So there is a need to add a protective resistor and to install a current limiting circuit to the bias circuit.

② A low-noise readout circuit usually has high input impedance, so the first stage might be damaged by excess voltage. To prevent this, a protective circuit should be connected to divert any excess input voltage to the power supply voltage line.

③ APD gain changes with temperature. To use an APD over a wide temperature range, the reverse voltage must be controlled to match the temperature changes or the APD temperature must be maintained at a constant level.

④ When detecting low-level light signals, the lower detection limit is determined by the shot noise. If background light enters the APD, then the S/N might deteriorate due to shot noise from background light. In this case, effects from background light must be minimized by using optical filters, improving laser modulation, and/or restricting the angle of view. Because of their structure, the excess noise index for InGaAs APDs is especially large compared to Si APD, so effects from shot noise including excess noise must be taken into account.

A connection example is shown in Figure 2-12.
We welcome requests for custom devices such as InGaAs APD modules (high-speed type, TE-cooled type, etc.).

[Figure 2-12] Connection example

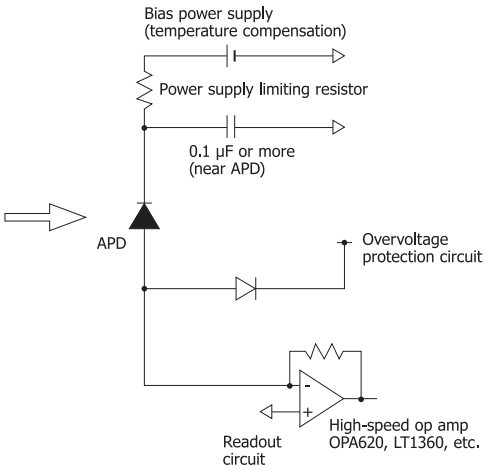


KIRDC0079EA

# 3. PbS/PbSe photoconductive detectors

PbS and PbSe photoconductive detectors are infrared detectors utilizing a photoconductive effect that lowers the electrical resistance when illuminated with infrared light. Compared to other detectors used in the same wavelength regions, PbS and PbSe photoconductive detectors offer the advantages of higher detection capability and operation at room temperature. However, the dark resistance, sensitivity, and response speeds change according to the ambient temperature, so caution is required.

## 3 - 1 Operating principle

When infrared light enters a PbS/PbSe photoconductive detector, the number of carriers increases, causing its resistance to lower. A circuit like that shown in Figure 3-1 is used to extract the signal as a voltage, and photo sensitivity is expressed in units of V/W.

[Figure 3-1] Output signal measurement circuit for photoconductive detector

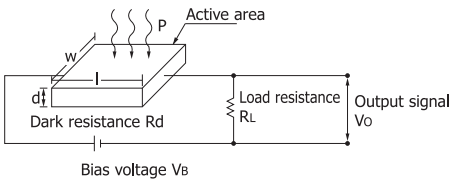


KIRDC0028EA

The output voltage (Vo) is expressed by equation (22).

$$Vo = \frac{RL}{Rd + RL} \cdot VB \quad \cdots\cdots (22)$$

The change (ΔVo) in Vo, which occurs due to a change (ΔRd) in the dark resistance (Rd) when light enters the detector, is expressed by equation (23).

$$\Delta Vo = - \frac{RL\ VB}{(Rd + RL)^2} \cdot \Delta Rd \quad \cdots\cdots (23)$$

ΔRd is then given by equation (24).

$$\Delta Rd = - Rd \frac{q(\mu e + \mu h)}{\sigma} \cdot \frac{\eta \tau \lambda P A}{l w d h c} \quad \cdots\cdots (24)$$

q : electron charge
μe : electron mobility
μh : hole mobility
σ : electric conductivity
η : quantum efficiency
τ : carrier lifetime
λ : wavelength
P : incident light level
A : active area
h : Planck's constant
c : speed of light in vacuum

## 3 - 2 Characteristics

### Spectral response

Temperature characteristics of PbS/PbSe band gap energy have a negative coefficient, so cooling the detector shifts its spectral response range to the long wavelength side.

[Figure 3-2] Spectral response

(a) PbS photoconductive detector

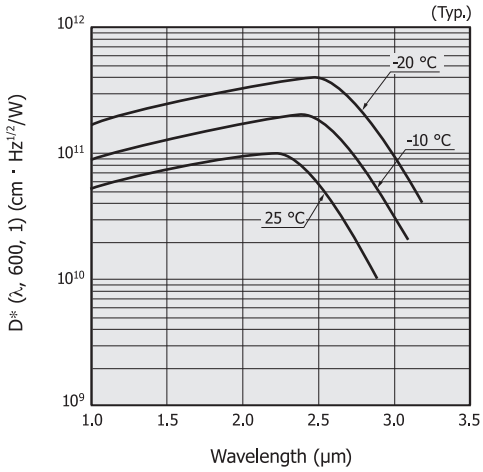


KIRDB0265EC

(b) PbSe photoconductive detector

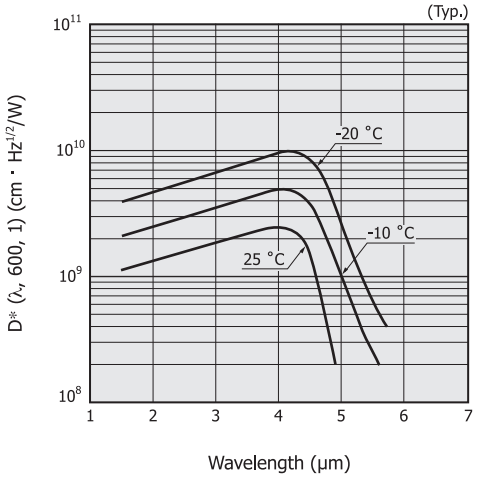


KIRDB0342EC

### Time response characteristics

Sensitivity frequency characteristic of PbS/PbSe photoconductive detectors is given by equation (25).

$$R(f) = \frac{R(o)}{\sqrt{1 + 4\pi^2 f^2 \tau^2}} \quad \cdots\cdots (25)$$

R(f) : frequency response
R(o) : response at zero frequency
f : chopping frequency
τ : time constant

Because PbS/PbSe photoconductive detector noise has a typical 1/f noise spectrum, D* is expressed by equation (26).

$$D^*(f) = \frac{k\sqrt{f}}{\sqrt{1+4\pi^2 f^2 \tau^2}} \text{ [V]} \cdots\cdots (26)$$

$D^*(f)$ is maximized at $f = \frac{1}{2\pi\tau}$ .

S/N frequency characteristics of PbS/PbSe photoconductive detectors are shown in Figure 3-3.

Sensitivity frequency characteristics of PbS photoconductive detectors at a room temperature (+25 °C) and at a TE-cooled temperature (-20 °C) are shown in Figure 3-4.

[Figure 3-3] S/N vs. chopping frequency

(a) PbS photoconductive detector

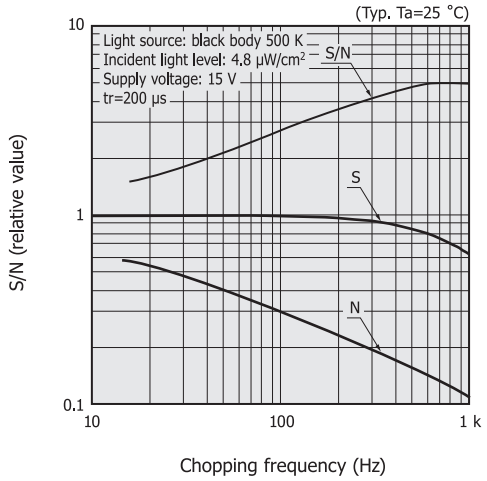


KIRDB0047EB

(b) PbSe photoconductive detector

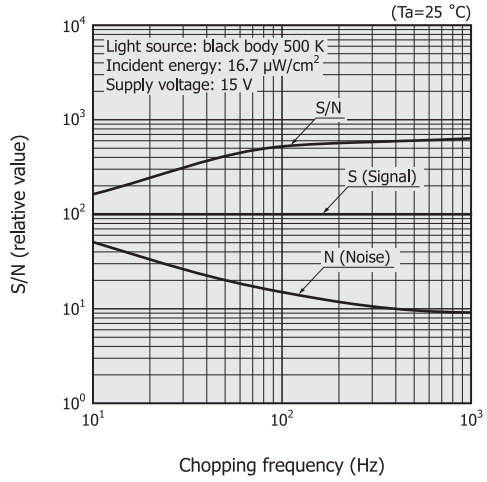


KIRDB0441EA

[Figure 3-4] Sensitivity vs. chopping frequency (PbS photoconductive detector)

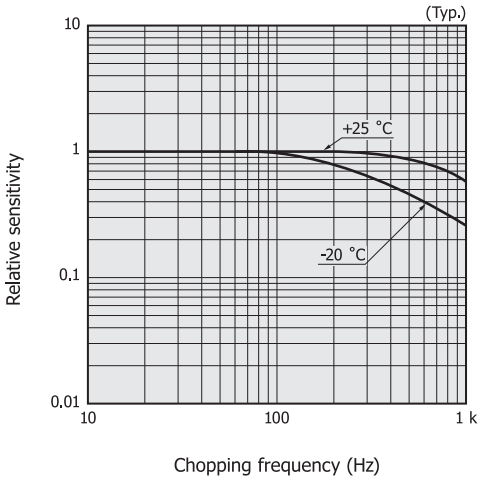


KIRDB0083EC

## Linearity

Figure 3-5 shows the relationship between incident light level and detector output. The lower linearity limits of PbS/PbSe photoconductive detectors are determined by their NEP.

[Figure 3-5] Linearity

(a) PbS photoconductive detector

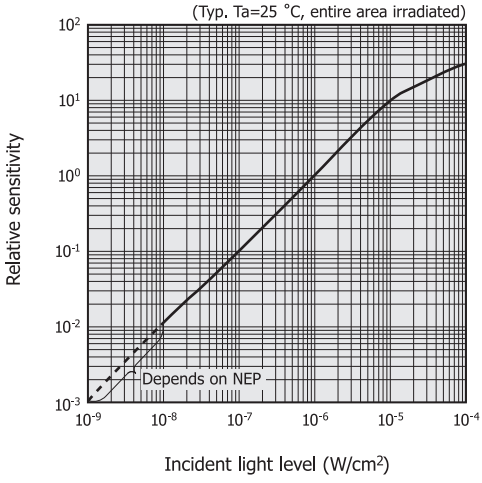


KIRDB0050EA

(b) PbSe photoconductive detector

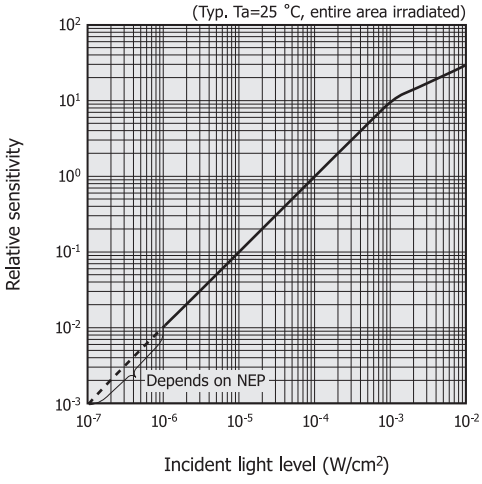


KIRDB0056EA

## Temperature characteristics

Photo sensitivity, dark resistance, and rise time of PbS/PbSe photoconductive detectors vary as the element temperature changes [Figures 3-6 and 3-7].

[Figure 3-6] Photo sensitivity vs. element temperature

(a) PbS photoconductive detector

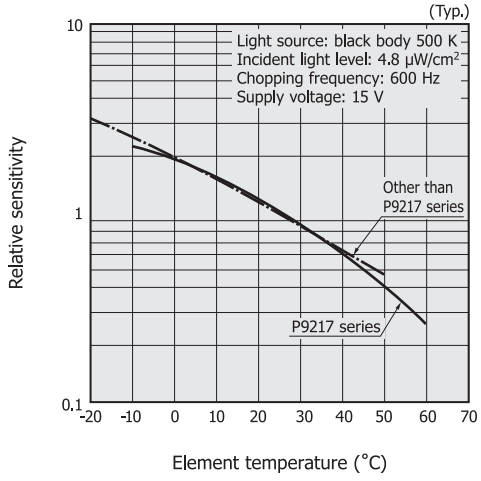


(b) PbSe photoconductive detector

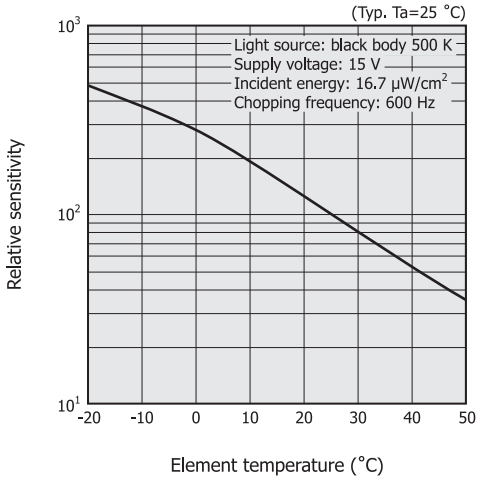


[Figure 3-7] Dark resistance and rise time vs. element temperature

(a) PbS photoconductive detector (P9217 series)

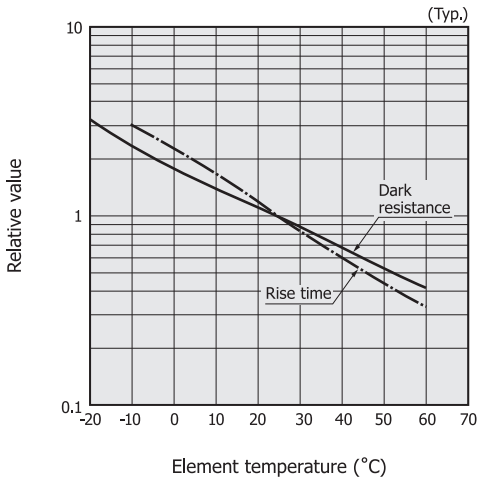


(b) PbSe photoconductive detector

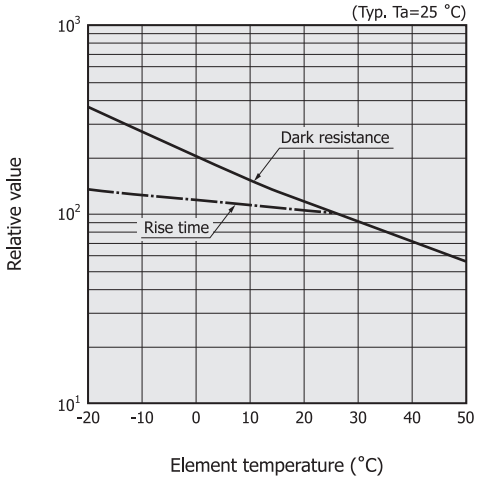


## 3 - 3 How to use

To operate PbS/PbSe photoconductive detectors, a chopper is usually used to acquire AC signals like the circuit shown in Figure 3-8.

[Figure 3-8] Connection example

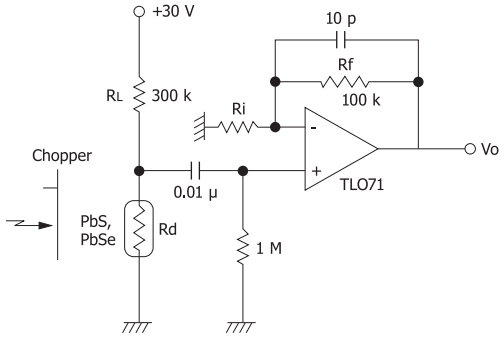


The signal voltage (Vo) in Figure 3-8 is expressed by equation (27).

$$Vo = -is \times Rd \left(1+\frac{Rf}{Ri}\right) \cdots\cdots\cdots (27)$$

is: signal current

## Temperature compensation

Since the sensitivity and dark resistance of PbS/PbSe photoconductive detectors drift according to the element temperature, some measures must be taken to control the temperature.

The HAMAMATSU TE-cooled PbS/PbSe photoconductive detectors contain a thermistor intended to maintain the element temperature at a constant level and to suppress the temperature-dependent drift. In some cases, the detectors are kept warmed at a constant temperature by a heater, etc. However, this may not only reduce sensitivity but also speed up deterioration in the detector so use caution.

## Load resistance

The largest signal can be obtained when the load resistance ($R_L$) and dark resistance (Rd) are the same value. The relationship between the output signal and $R_L$/Rd is shown in Figure 3-9.

[Figure 3-9] Output vs. $R_L$/Rd

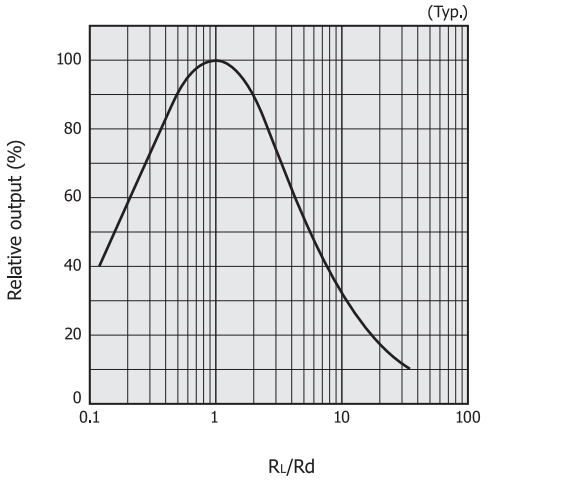


## Chopping frequency

As stated in "Time response characteristics" in section 3-2, "Characteristics," the D* is maximized at $f = \frac{1}{2\pi\tau}$. Narrowing the amplifier bandwidth will reduce the noise and improve the S/N. In low-light level measurement, the chopping frequency and bandwidth must be taken into account.

## Voltage dependence

The noise of PbS/PbSe photoconductive detectors suddenly increases when the voltage applied to the detector exceeds a certain value. Though the signal increases in proportion to the voltage, the detector should be used at as low a voltage as possible within the maximum supply voltage listed in our datasheets.

## Active area size

To obtain a better S/N, using a small-area PbS/PbSe photoconductive detector and narrowing the incident light on the detector to increase the light level per unit area on the detector prove more effective than using a large-area detector. If the incident light deviates from the active area or light other than signal light strikes the detector, this may lower the S/N, so use extra caution to avoid these problems.

## Precautions for use (PbS photoconductive detectors)

Characteristics of PbS photoconductive detectors may change if stored at high temperatures or under visible light (room illumination) or ultraviolet light, etc. Always store these detectors in a cool, dark place. If these detectors are used under visible light, etc., then provide light-shielding to block that light.

# 4. InSb photoconductive detectors

InSb photoconductive detectors are infrared detectors capable of detecting light up to approx. 6.5 µm. InSb photoconductive detectors are easy to handle since they are thermoelectrically cooled (liquid nitrogen not required).

[Figure 4-1] Spectral response (P6606-310)

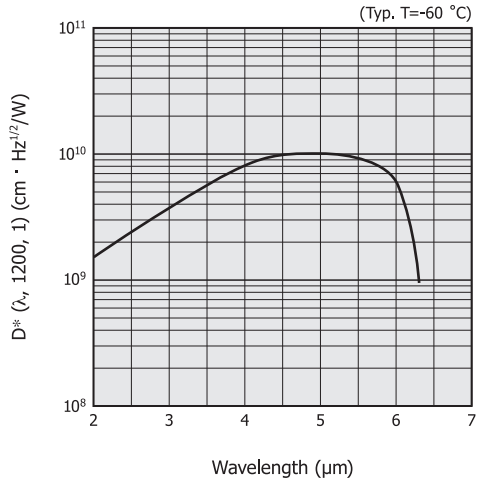


The band gap energy in InSb photoconductive detectors has a positive temperature coefficient, so cooling the detector shifts its cut-off wavelength to the short-wavelength side. This is the same for InSb photovoltaic detectors.

[Figure 4-2] D* vs. element temperature (P6606-310)

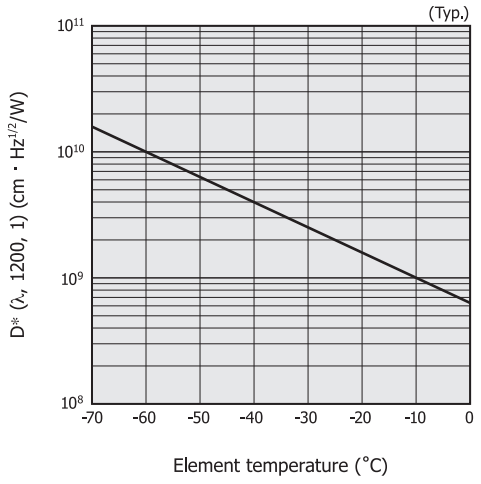


# 5. InAs/InSb photovoltaic detectors

As with InGaAs PIN photodiodes, InAs and InSb photovoltaic detectors are photovoltaic devices having a PN junction. InAs photovoltaic detectors are sensitive around 3 µm, the same as PbS photoconductive detectors, while InSb photovoltaic detectors are sensitive to the 3 to 5 µm band, the same as PbSe photoconductive detectors.
InAs/InSb photovoltaic detectors offer fast response and a high S/N and so are used in applications different from those for PbS/PbSe photoconductive detectors.

## 5 - 1 Characteristics

### Spectral response

InAs photovoltaic detectors include a non-cooled type, TE-cooled type, and liquid nitrogen cooled type which are used for different applications and purposes.
InSb photovoltaic detectors are only available as liquid nitrogen cooled types. Figure 5-1 shows spectral responses of InAs/InSb photovoltaic detectors.

[Figure 5-1] Spectral response
(a) InAs photovoltaic detector

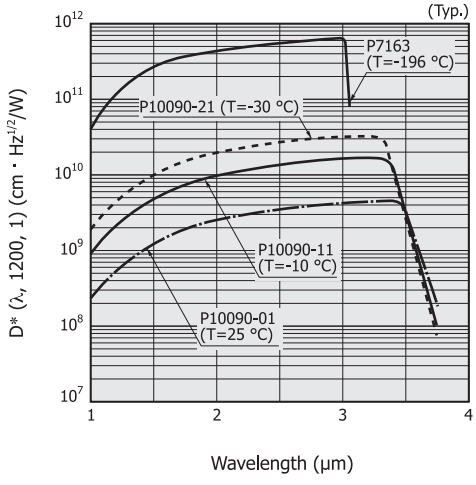

(b) InSb photovoltaic detector

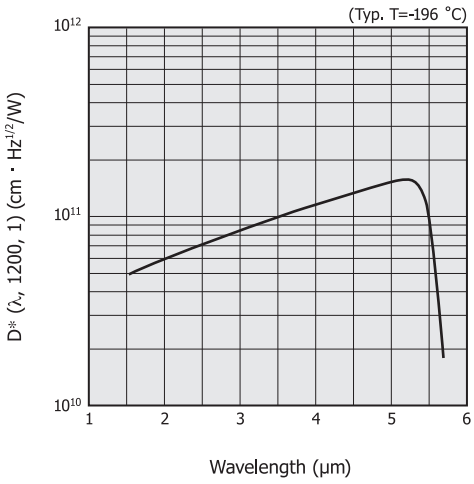


## Noise characteristics

InAs/InSb photovoltaic detector noise (i) results from Johnson noise (ij) and shot noise ($i_{SD}$) due to dark current (including photocurrent generated by background light). Each type of noise is expressed by the following equations:

$$i = \sqrt{ij^2 + i_{SD}^2} \quad \cdots\cdots\cdots\cdots (28)$$

$$ij = \sqrt{4k\,T\,B\,/\,Rsh} \quad \cdots\cdots\cdots (29)$$

$$i_{SD} = \sqrt{2q\,I_D\,B} \quad \cdots\cdots\cdots\cdots (30)$$

k : Boltzmann's constant
T : absolute temperature of element
B : noise bandwidth
Rsh : shunt resistance
q : electron charge
$I_D$ : dark current

When considering the spectral response range of InSb photovoltaic detectors, background light fluctuations (background radiation noise) from the surrounding areas cannot be ignored. The D* of InSb photovoltaic detectors is given by equation (31) assuming that the background radiation noise is the only noise source.

$$D^* = \frac{\lambda\sqrt{\eta}}{h\,c\sqrt{2Q}} \ [cm \cdot Hz^{1/2}/W] \quad \cdots\cdots\cdots (31)$$

λ : wavelength
η : quantum efficiency
h : Planck's constant
c : speed of light
Q: background photon flux [photons/cm$^2$·s]

To reduce background radiation noise, the detector's field of view (FOV) must be limited by using a cold shield or unwanted wavelengths must be eliminated by using a cooled band-pass filter. Figure 5-3 shows how the D* relates to the field of view.

[Figure 5-2] Field of view (FOV)

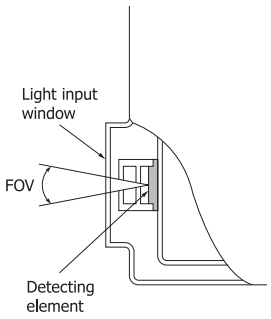


[Figure 5-3] D* vs. field of view

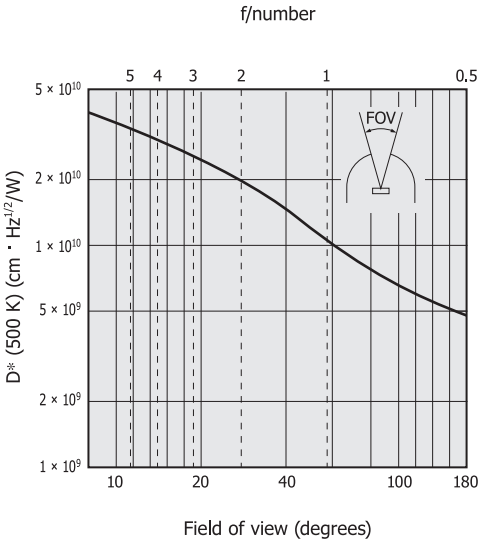


# 5 - 2 Precautions

## Resistance measurement

Measuring the resistance of InAs/InSb photovoltaic detectors with a multimeter might damage the detector. This risk is even higher at room temperature, so always cool the detector when making this measurement. The bias voltage applied to the detector at this time must be within the absolute maximum rating.

## Input of visible light (InSb photovoltaic detector)

When visible light or ultraviolet light with energy higher than infrared light enters the InSb photovoltaic detector, an electric charge accumulates on the surface of the element, causing the dark current to increase. The increased dark current also increases noise to degrade the S/N level. Before using, put a cover (such as a double layer of black tape) over the light input window to prevent visible light (room illumination) or ultraviolet, etc. from entering the element. Then pour liquid nitrogen into the dewar. If the detector has been exposed

to visible light, etc. after pouring liquid nitrogen and the dark current has increased, remove the liquid nitrogen from the dewar to return the element temperature back to room temperature. Then redo the above procedure, and the dark current will return to the previous level.

# 6. MCT (HgCdTe) photoconductive detectors

MCT (HgCdTe) photoconductive detectors are infrared detectors whose resistance decreases when illuminated with infrared light. These detectors are mainly used for infrared detection around 5 µm and 10 µm.

## 6 - 1 Characteristics

### Spectral response

The band gap energy of HgCdTe crystal varies according to the composition ratio of HgTe and CdTe. This means that infrared detectors having peak sensitivity at different wavelengths can be fabricated by changing this composition ratio. The relation between band gap energy and cut-off wavelength is shown in equation (32).

$$\lambda c = \frac{1.24}{Eg} \cdots\cdots (32)$$

λc: cut-off wavelength [µm]
Eg: band gap energy [eV]

Besides the composition ratio, the band gap energy also varies depending on the element temperature.

$$Eg = 1.59X - 0.25 + 5.23 \times 10^{-4} T (1 - 2.08X) + 0.327X^3 \cdots\cdots (33)$$

X: indicates the $Hg_{1-x}CdxTe$ composition ratio
T: absolute temperature

The band gap energy increases as the element temperature rises, causing the peak sensitivity wavelength to shift to the short wavelength side.
Figure 6-2 shows spectral responses of MCT photoconductive detectors.

[Figure 6-1] Band gap energy vs. MCT crystal composition ratio

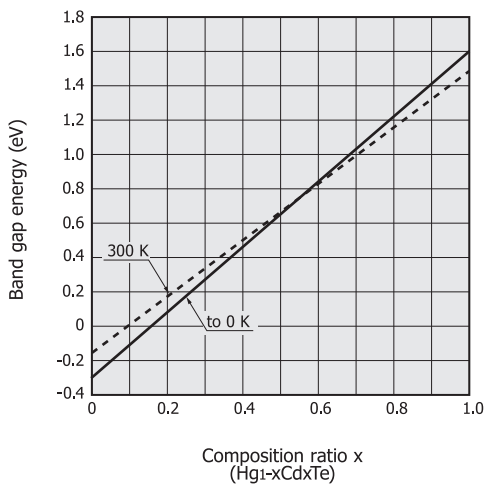


KIRDB0087EA

[Figure 6-2] Spectral response (MCT photoconductive detector)

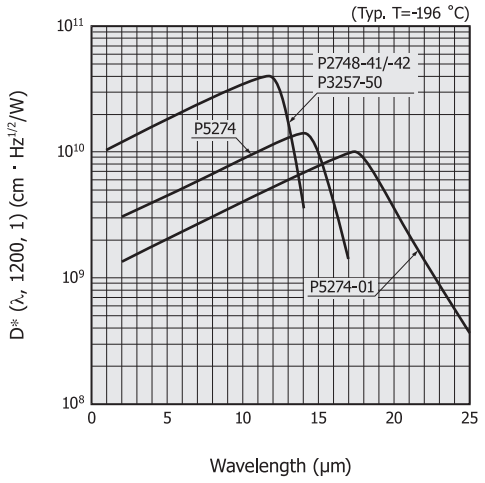




## Noise characteristics

Noise components in MCT photoconductive detectors include 1/f noise, g-r noise caused by electron-hole recombination, and Johnson noise. The 1/f noise is predominant at low frequencies below several hundred hertz, and the g-r noise is predominant at frequencies higher than that level. Figure 6-3 shows the relationship between the noise level and frequency for an MCT photoconductive detector. In MCT photoconductive detectors with sensitivity at wavelengths longer than 3 µm, fluctuations in background light at 300 K appear as noise and cannot be ignored. But this noise can be reduced by narrowing the field of view.

[Figure 6-3] Noise level vs. frequency (MCT photoconductive detector)

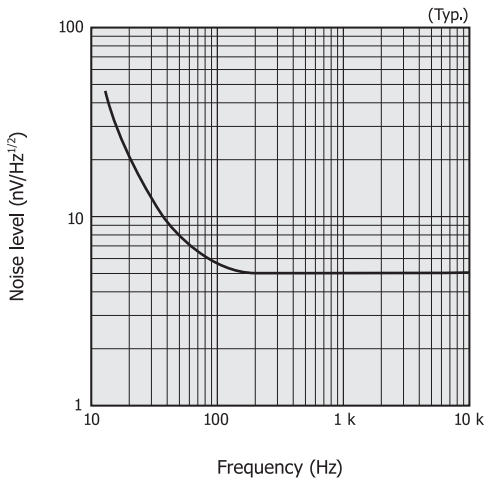


## Temperature characteristics

The D* and spectral response of MCT photoconductive detectors vary according to the element temperature. As the temperature rises, the D* decreases and the spectral response range shifts to the short-wavelength side. As examples of this, Figures 6-4 and 6-5 show temperature characteristics of D* and cut-off wavelength, using an MCT photoconductive detector P2750 for the 3 to 5 µm band.

[Figure 6-4] D* vs. element temperature (P2750)

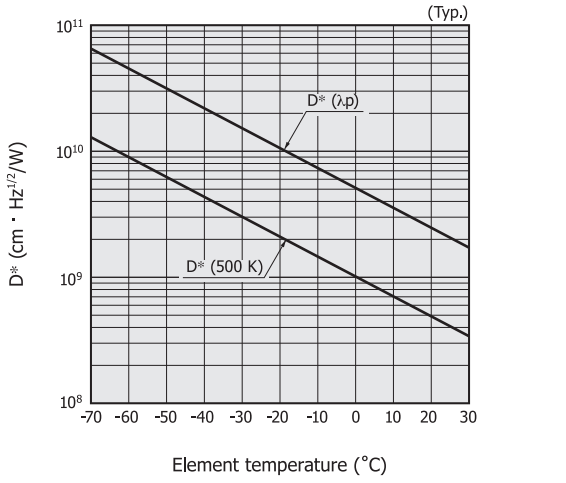


[Figure 6-5] Cut-off wavelength vs. element temperature (P2750)

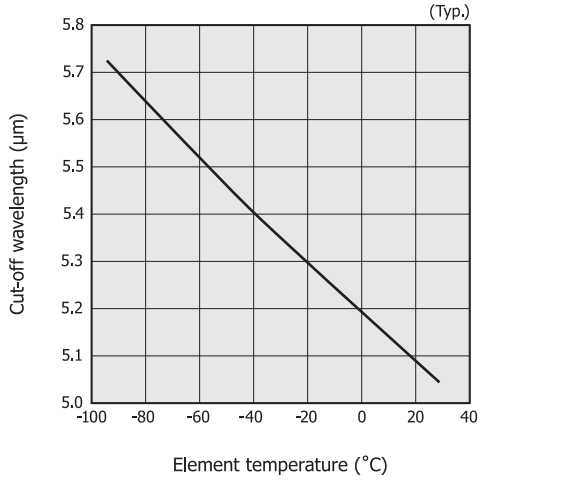


## Linearity

[Figure 6-6] Linearity (P3257-25/-01/-10)

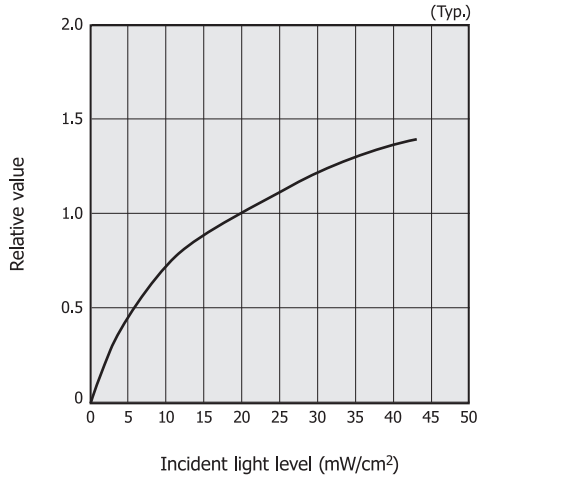

## 6-2 How to use

### Operating circuit

Figure 6-7 shows a connection example for MCT photoconductive detectors. A power supply with low noise and ripple should be used. A load resistance ($R_L$) of several kilohms is generally used to make it a constant current source. As the bias current is raised, both the signal and noise increase [Figure 6-8]. But the noise begins to increase sharply after reaching a particular value, so the bias current should be used in a range where the D* becomes constant. Raising the bias current more than necessary increases the element temperature due to Joule heat and degrades the D*. This might possibly damage the detector so it should be avoided.

[Figure 6-7] Connection example (MCT photoconductive detector)

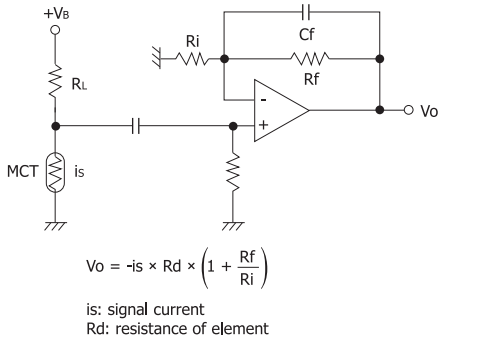


KIRDC0021EA

[Figure 6-8] Signal, noise, and D* vs. bias current (P3257-10, typical example)

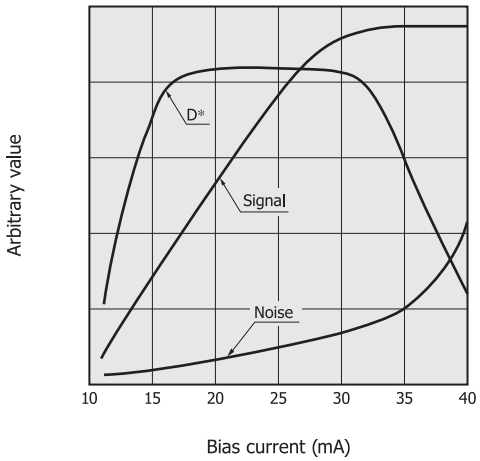


KIRDB0091EB

### Ambient temperature

MCT photoconductive detector sensitivity varies with the ambient temperature. As the ambient temperature rises, the background radiation noise increases and the number of carriers in the element also increases. This shortens the average lifetime of the carriers excited by signal light, resulting in lower sensitivity.

# 7. MCT (HgCdTe) photovoltaic detectors

MCT photovoltaic detectors are infrared detectors utilizing the photovoltaic effect that generates photocurrent when illuminated with infrared light, the same as InAs photovoltaic detectors. These MCT photovoltaic detectors are mainly used for infrared detection around 10 µm.

## 7-1 Characteristics

### Spectral response

[Figure 7-1] Spectral response (MCT photovoltaic detector)

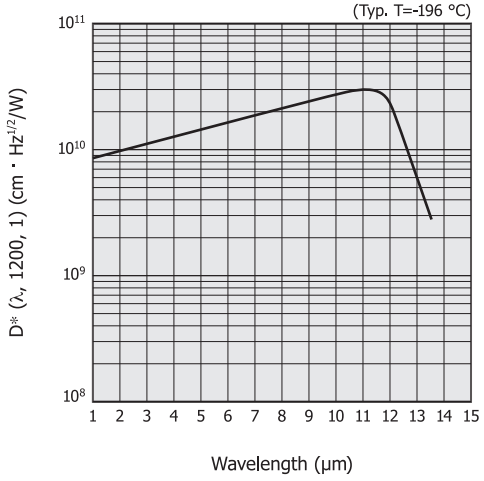


KIRDB0334EB

### Noise characteristics

To find information on photovoltaic detector noise characteristics, see “5-1 Characteristics/Noise characteristics” in section 5, “InAs/InSb photovoltaic detectors.” Compared to photoconductive detectors, photovoltaic detectors have smaller 1/f noise and are therefore advantageous for measuring light at low frequencies.

### Linearity

The upper linearity limit of MCT photovoltaic detectors is one order of magnitude or more higher than that (several mW/cm$^2$) of MCT photoconductive detectors.

[Figure 7-2] Linearity (MCT photovoltaic detector)

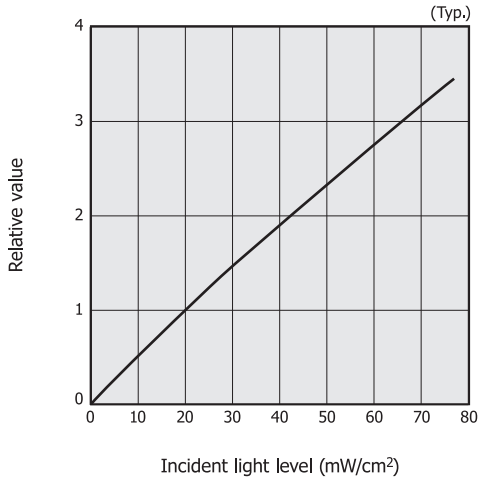


KIRDB0404EA

## 7-2 How to use

### Operating circuit

Figure 7-3 shows a connection example for MCT photovoltaic detectors. The photocurrent is extracted as a voltage using a load resistor or op amp.

[Figure 7-3] Connection example (MCT photovoltaic detector)

(a) With load resistor connected

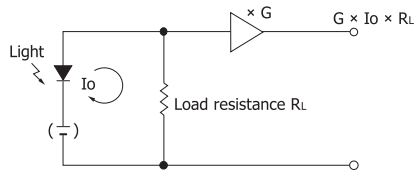


(b) With op amp connected

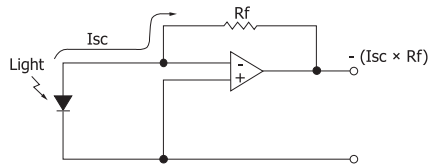


KPDC0006EC

### Ambient temperature

In MCT photovoltaic detector operation, if the background radiation noise changes due to ambient temperature fluctuations, then the dark current also changes. To prevent this phenomenon, pay careful attention to optical system design. For example use a properly shaped cold shield that does not allow pickup of unnecessary background light.

## 8. Two-color detectors

Two-color detectors are infrared detectors that use two or more vertically stacked detectors to extend the spectral response range. A Si photodiode is usually mounted as the light incident surface over a PbS or PbSe or InGaAs detector along the same optical axis. A combination of InAs and InSb or of InSb and MCT (HgCdTe) can also be used for the same purpose. The upper detector not only detects infrared light but also serves as a short-wavelength cut-off filter for the lower detector.

[Figure 8-1] Dimensional outline
[two-color detector (Si + InGaAs), unit: mm]

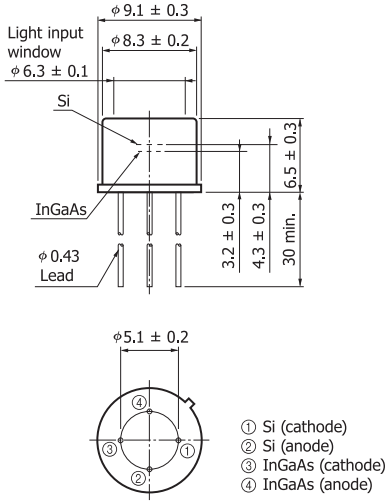


KIRDA0147EB

[Figure 8-2] Spectral response [two-color detector (Si + InGaAs)]

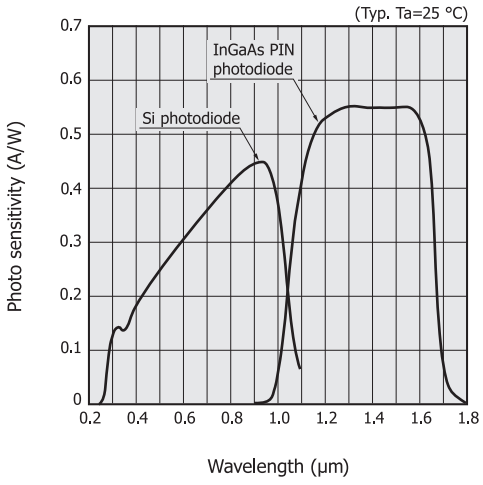


KIRDB0405EA

# 9. New approaches

## 9 - 1 High-speed InGaAs PIN photodiodes

As fast response photosensors, the product demand for 20 Gbps and 40 Gbps photodiodes is on the rise. In this case, it is essential to keep the cost of the system itself from rising, so low power consumption and ease of assembling are simultaneously required. To meet these needs, the photodiodes must operate at high speed under a low reverse voltage and the manufacturing process must integrate optical techniques to guide as much light as possible into a small active area. We have developed a high-speed InGaAs PIN photodiode prototype that operates from a small reverse voltage and verified its operation on transmission bands up to 25 Gbps at $V_R$=2 V.

[Figure 9-1] Frequency characteristic (high-speed InGaAs PIN photodiode)

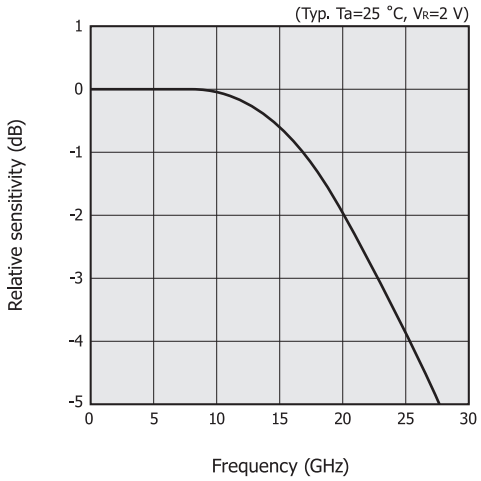


KIRDB0394EA

## 9 - 2 InAsSb photodiodes

InAsSb is a mixed crystal of InAs and InSb, and its band gap energy and peak sensitivity wavelength can be varied by changing the composition ratio [Figure 9-2]. This means that various types of infrared detectors with different spectral ranges can be fabricated by changing the composition ratio. PbSe and HgCdTe are other infrared detectors used in similar spectral response ranges as InAsSb. Unlike these materials, InAsSb is environmentally friendly and so is not subject to the RoHS directive. Moreover, the InAsSb photodiode employs a planar structure that delivers both high sensitivity and high reliability.

Utilizing the features of the new InAsSb material, we are expanding the spectral response range up to 12 µm, in order to cover wavelengths (approx. 10 µm) at human body temperatures while maintaining high sensitivity and high reliability. We are also developing easy-to-use sensors that operate at room temperature or by thermoelectric cooling, as well as two-dimensional image sensors, etc.

[Figure 9-2] Band gap energy and peak sensitivity wavelength vs. composition ratio x of $InAs_xSb_{1-x}$

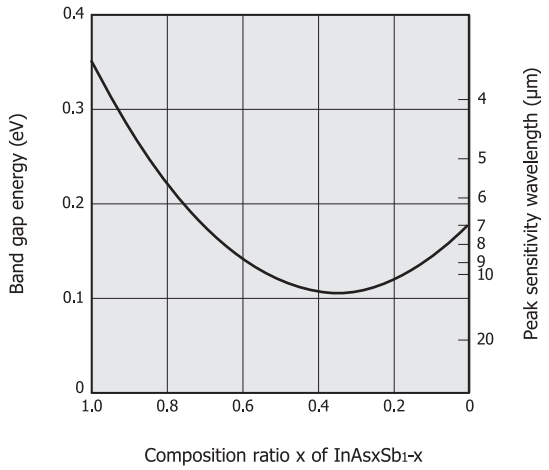


KIRDB0406EA

[Figure 9-3] Spectral response (InAsSb photodiode)

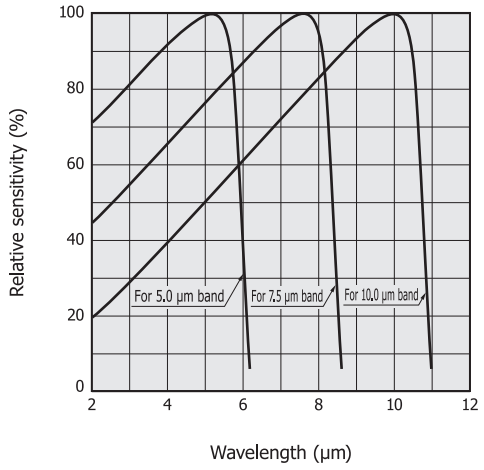


KIRDB0407EA

# 10. Applications

## 10 - 1 Optical power meters

Optical power meters measure light level and are used in a wide range of applications including optical fiber communications and laser beam detection. Optical fiber communications are grouped into two categories: short/middle distance and long distance communications. In long distance communications, infrared light in the 1.3 and 1.5 µm wavelength regions has less optical loss during transmission through optical fibers. In these wavelength regions, InGaAs PIN photodiodes are used to measure transmission loss in optical fibers, check whether relays are in satisfactory condition, and measure laser power. Major characteristics required of optical power meters are linearity and uniformity. In some cases, cooled type detectors are used to reduce the noise levels so that even low-power light can be detected.

## 10 - 2 LD monitors

The output level and emission wavelength of LD (laser diodes) vary with the LD temperature. So APC (automatic power control) is used to stabilize the LD. APC includes two methods. One method monitors the integrated amount of light pulses from the LD, and the other monitors the peak values of light pulses. Along with the steady increase in LD output power, linearity at higher light levels has become important for the detectors used in these monitors. High-speed response is also required to monitor the peak values of light pulses.
InGaAs PIN photodiodes used for LD monitors are mounted either in the same package as the LD or outside the LD package. Also, InAs and InSb photovoltaic detectors are used to monitor lasers at even longer wavelengths.

## 10 - 3 Radiation thermometers

Any object higher than absolute zero degrees radiates infrared light matching its own temperature. The quantity of infrared light actually emitted from an object is not directly determined just by the object temperature but must be corrected according to the object's emissivity (e).
Figure 10-1 shows the radiant energy from a black body. The black body is e=1. Figure 10-2 shows the emissivity of various objects. The emissivity varies depending on temperature and wavelength.
The noise equivalent temperature difference (NEΔT) is used as one measure for indicating the temperature resolution. NEΔT is defined in equation (34).

$$NE\Delta T = \frac{L_N}{\left.\frac{dL}{dT}\right|_{T=T_1}} \quad \cdots\cdots (34)$$

$L_N$: noise equivalent luminance
$T_1$: temperature of object
$L$ : radiance of object

Noise equivalent luminance ($L_N$) relates to the detector NEP as shown in equation (35).

$$NEP = To\, L_N\, \Omega\, Ao / \gamma \quad \cdots\cdots (35)$$

To : optical system loss
Ω : solid angle from optical system toward measurement area
Ao: aperture area of optical system
γ : circuit system loss

$\left.\frac{dL}{dT}\right|_{T=T_1}$ in equation (34) represents the temperature coefficient of radiant luminance from an object at temperature $T_1$. The radiant luminance can be obtained by integrating the spectral radiant exitance over the wavelength range ($\lambda_1$ to $\lambda_2$) being observed.

$$L = \int_{\lambda_1}^{\lambda_2} \frac{1}{\pi} M_\lambda \, d\lambda \quad \cdots\cdots (36)$$

$M_\lambda$: spectral radiant exitance

Radiation thermometers offer the following features compared to other temperature measurement methods.

· Non-contact measurement avoids direct contact with object.
· High-speed response
· Easy to make pattern measurements

Infrared detectors for radiation thermometers should be selected according to the temperature and material of the object to be measured. For example, peak emissivity wavelength occurs at around 5 µm in glass materials and around 3.4 µm or 8.4 µm in plastic films, so a detector sensitive to these wavelength regions must be selected.
Infrared detectors combined with an infrared fiber now make it possible to measure the temperature of objects in hazardous locations such as hot metal detectors (HMD), rotating objects, complex internal structures, and objects in a vacuum or in high-pressure gases.

[Figure 10-1] Black body radiation law (Planck's law)

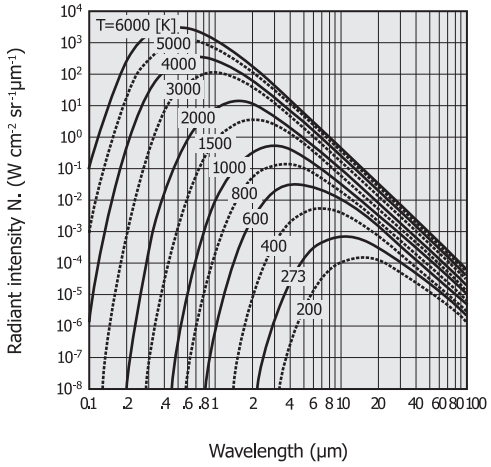


KIRDB0014EB

[Figure 10-2] Emissivity of various objects

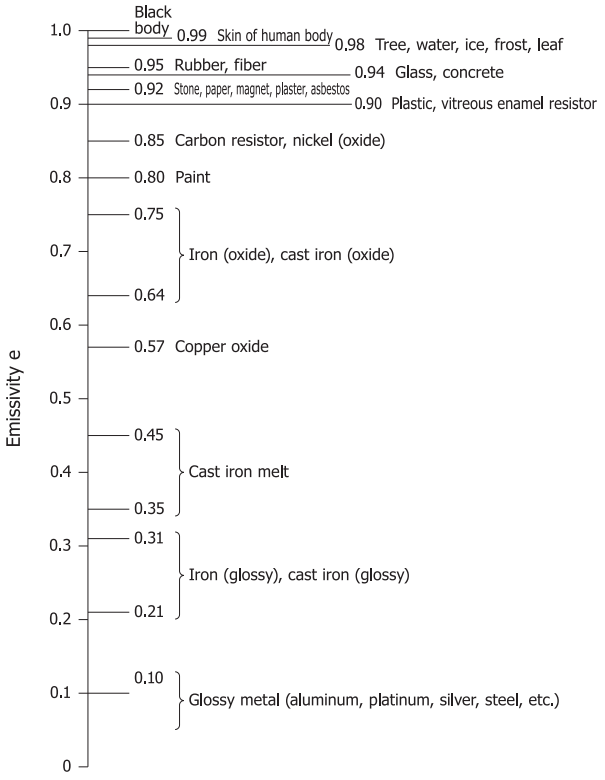


KIRDC0036EA

[Figure 10-3] Spectral transmittance and reflectance of glass

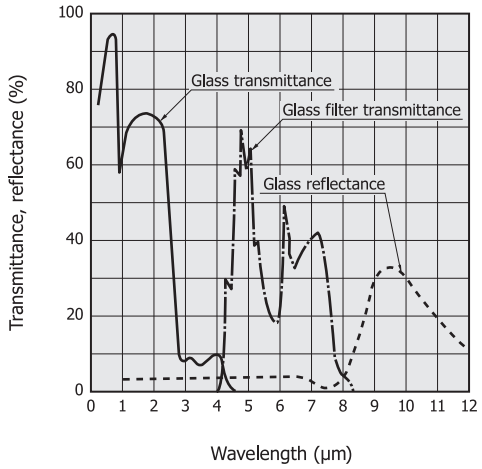


KIRDB0146EA

## 10 - 4 Flame eyes (flame monitors)

Flame monitors detect light emitted from flames to monitor the flame burning state. Radiant wavelengths from flames cover a broad spectrum from the ultraviolet to infrared region as shown in Figure 10-4. Flame detection methods include detecting infrared light using a PbS photoconductive detector, detecting a wide spectrum of light from ultraviolet to infrared using a two-color detector (Si + PbS), and detecting the 4.3 μm wavelength using a PbSe photoconductive detector.

[Figure 10-4] Radiant spectrum from flame

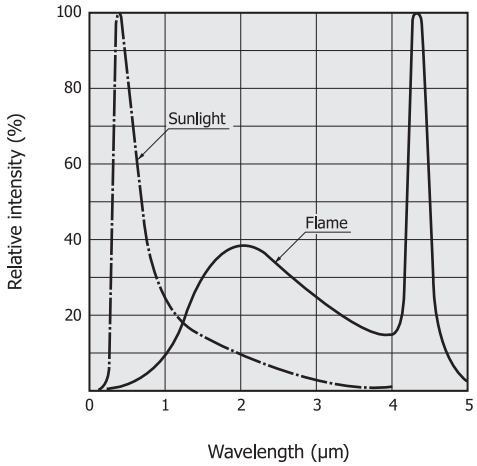


KIRDB0147EA

## 10 - 5 Moisture meters

Moisture meters measure the moisture of objects such as plants or mineral coals by illuminating the object with reference light and with near infrared light at water absorption wavelengths (1.1 μm, 1.4 μm, 1.9 μm, 2.7 μm). The two types of light reflected from or transmitted through the object are detected, and their ratio is calculated to measure the moisture level of the object. Photosensors suited for moisture measurement include InGaAs PIN photodiodes, InAs photovoltaic detectors, and PbS

photoconductive detectors.

## 10 - 6 Gas analyzers

Gas analyzers measure gas concentrations by making use of the fact that gases absorb specific wavelengths of light in the infrared region. Gas analyzers basically utilize two methods: a dispersive method and a non-dispersive method. The dispersive method disperses infrared light from a light source into a spectrum and measures the absorption amount at each wavelength to determine the constituents and quantities of the sample. The non-dispersive method measures the absorption amounts only at particular wavelengths. The non-dispersive method is currently the method mainly used for gas analysis. Non-dispersive method gas analyzers are used for measuring automobile exhaust gases (CO, CH, $CO_2$) and exhaled respiratory gas components ($CO_2$), as well as for regulating fuel exhaust gases (COx, SOx, NOx) and detecting fuel leaks ($CH_4$, $C_2H_6$). Further applications include $CO_2$ (4.3 µm) measurements in carbonated beverages (soft drinks, beer, etc.) and sugar content (3.9 µm) measurement. Figure 10-5 shows absorption spectra of various gases.
HAMAMATSU provides InGaAs, InAs, InSb, PbS, PbSe, and MCT, etc. as sensors to measure the various light wavelengths.

[Figure 10-5] Gas absorption spectra

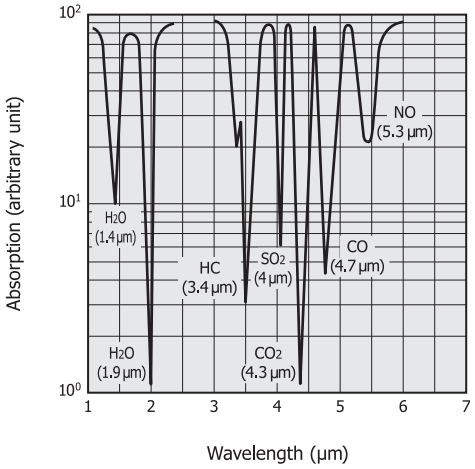


KIRDB0148EA

## 10 - 7 Infrared imaging devices

Infrared imaging devices are finding a wide range of applications from industry to medical imaging, academic research, and many other fields [Table 10-1]. The principle of infrared imaging is grouped into two techniques [Figure 10-6]. One technique uses a one-dimensional array that captures an image by scanning the optical system along the Z axis. The other technique uses a two-dimensional array and so does not require scanning the optical system.
Even higher quality images can be acquired with InSb or MCT photoconductive/photovoltaic detectors, QWIP (quantum well infrared photodetector), thermal detectors utilizing MEMS technology, and two-dimensional arrays fabricated by heterojunction to CMOS circuitry.

[Figure 10-6] Principles of infrared imaging device
(a) Scanning using one-dimensional array

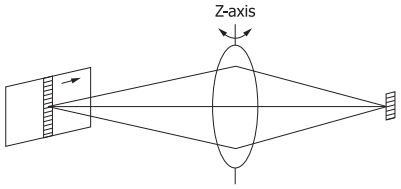


(b) Electronic scanning by two-dimensional array

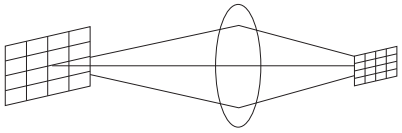

KIRDC0037EB

## 10 - 8 Remote sensing

Light emitted or reflected from objects contains different information depending on the wavelength as shown in Figure 10-7. Measuring this light at each wavelength allows obtaining various information specific to the object. Among the various measurements, infrared remote sensing can acquire information such as the surface temperature of solids or liquids, or the type and temperature of gases. Remote sensing from space satellites and airplanes is recently becoming increasingly used to obtain

[Table 10-1] Infrared imaging device application fields

| Application field | Application example |
|---|---|
| Industry | Process control for steel and paper, non-destructive inspection of welds or soldering, non-destructive inspection of buildings and structures, evaluating wafers and IC chips, inspecting and maintaining power transmission lines and electric generators, heat monitoring of shafts and metal rolling, marine resource surveys, forest distribution monitoring |
| Pollution monitor | Monitoring of seawater pollution and hot wastewater |
| Academic research | Geological surveys, water resource surveys, ocean current research, volcano research, meteorological investigations, space and astronomical surveys |
| Medical imaging | Infrared imaging diagnosis (diagnosis of breast cancer, etc.) |
| Security and surveillance | Monitoring of boiler temperatures, fire detection |
| Automobile, airplane | Night vision device for visual enhancement, engine evaluations |

global and macroscopic information such as the temperature of the earth's surface or sea surface and the gas concentration in the atmosphere. Information obtained in this way is utilized for environmental measurement, weather observation, and resource surveys.

[Figure 10-7] Optical system for resource survey

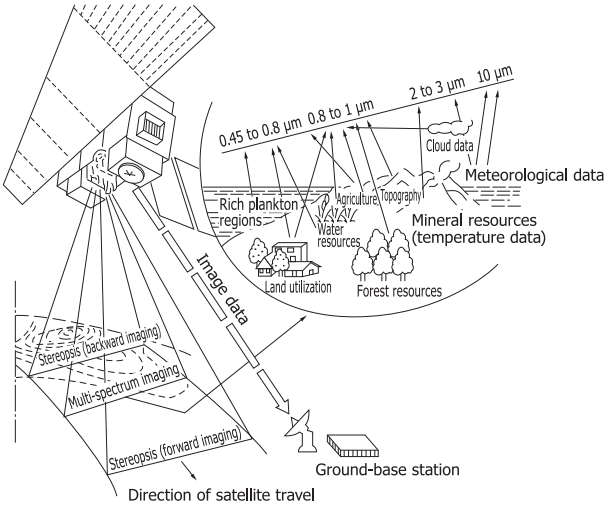


KIRDC0039EB

## 10 - 9 Sorting machines

Making use of the absorption wavelengths inherent to organic matter allows sorting it into organic and inorganic matter. Agricultural crops such as rice, potatoes, tomatoes, onions, and garlic are distinguished from clods and stones based on this principle by using InGaAs PIN photodiodes and PbS photoconductive detectors. These infrared detectors also detect differences in temperature, emissivity, and transmittance of objects carried on a conveyor in order to sort fruits for example by sugar content or to separate waste such as plastic bottles for recycling.

## 10 - 10 FT-IR

The FT-IR (Fourier transform - infrared spectrometer) is an instrument that acquires a light spectrum by Fourier-transforming interference signals obtained with a double-beam interferometer. It has the following features:

· High power of light due to non-dispersive method (simultaneous measurement of multiple spectral elements yields high S/N)
· High wavelength accuracy

The following specifications are required for infrared detectors that form the core of the FT-IR.

· Wide spectral response range
· High sensitivity
· Active area size matching the optical system
· Wide frequency bandwidth
· Excellent linearity versus incident light level

Thermal type detectors are generally used over a wide spectral range from 2.5 µm to 25 µm. Quantum type detectors such as MCT, InAs, and InSb are used in high-sensitivity and high-speed measurements.
Usage of InGaAs and InAs has also extended the spectral range to the near infrared region. One-dimensional or two-dimensional arrays such as MCT and InSb are used for infrared mapping and infrared imaging spectrometry.

深圳商斯达实业**专用电路与单片机部**是专业开发、设计、生产、代理、经销专用电路（ASIC）和单片机配套产品，温度、湿度、语音、报警、计时、计步、测速、调光、游戏、新特优等专用芯片和模组；专用电路、微控制器、DSP、语音系统开发、设计、测试、仿真工具，为消费电子、通信、家电、防盗报警厂家提供专业服务。产品主要有：1、温度计电路、体温计电路、湿度计电路、时钟温湿度计电路、计时钟控电路、计步运动表电路、测速电路、调光电路、游戏电路、防盗报警电路、遥控电路、钟表电路、闪灯电路、计数电路、语音电路等专用芯片和模组，为三资企业、外贸出口企业提供完整配套服务；2、带 LED 闪烁电路、声效电路、玩具钢琴电路、音乐音效电路、灯串电路、风扇控制电路、计算器电路、万年历电路、汇率转换电路、玩具声光电路、遥控编解码电路、红外线遥控电路、无线遥控电路及配件、语音录放电路、圣诞灯电路、热释电控制器（人体感应）电路等专用芯片和配套模组.


更多产品请看本公司产品专用销售网站:

商斯达中国传感器科技信息网：http://www.sensor-ic.com/

商斯达工控安防网：http://www.pc-ps.net/

商斯达电子 元器件网：http://www.sunstare.com/

商斯达微波光电产品网:HTTP://www.rfoe.net/

商斯达消费电子产品网://www.icasic.com/

商斯达实业科技产品网://www.sunstars.cn/

传感器销售热线：

地址：深圳市福田区福华路福庆街鸿图大厦 1602 室

电话：0755-83387016 83387030 83398389 83600266

传真：0755-83376182 （0）13902971329 MSN: SUNS8888@hotmail.com

邮编：518033 E-mail:szss20@163.com QQ: 195847376

深圳赛格展销部：深圳华强北路赛格电子市场 2583 号 电话：0755-83665529 25059422

技术支持：0755-83394033 13501568376


欢迎索取免费详细资料、设计指南和光盘 ；产品凡多，未能尽录，欢迎来电查询。


北京分公司：北京海淀区知春路 132 号中发电子大厦 3097 号

TEL：010-81159046 82615020 13501189838 FAX：010-62543996

上海分公司：上海市北京东路 668 号上海赛格电子市场 2B35 号

TEL：021-28311762 56703037 13701955389 FAX：021-56703037

西安分公司：西安高新开发区 20 所(中国电子科技集团导航技术研究所)

西安劳动南路 88 号电子商城二楼 D23 号

TEL：029-81022619 13072977981 FAX:029-88789382